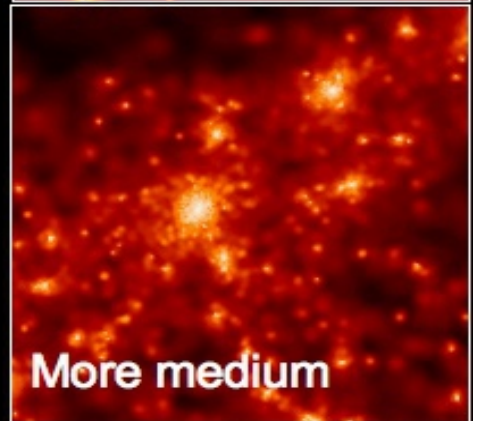# Analysis of Dark Matter Simulations
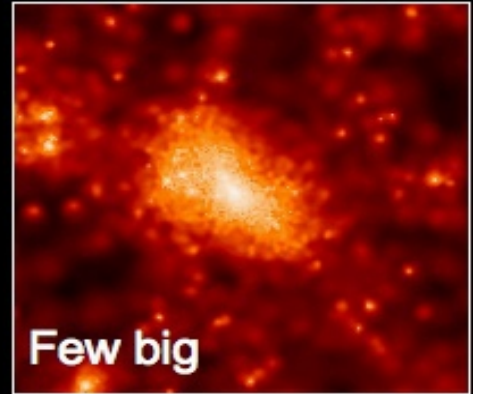

The Web of Dark Matter Halos

Few big

More medium

Many small
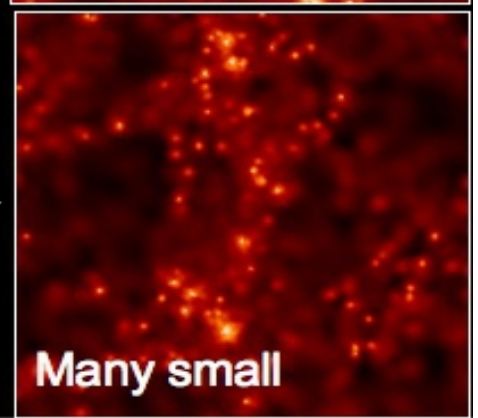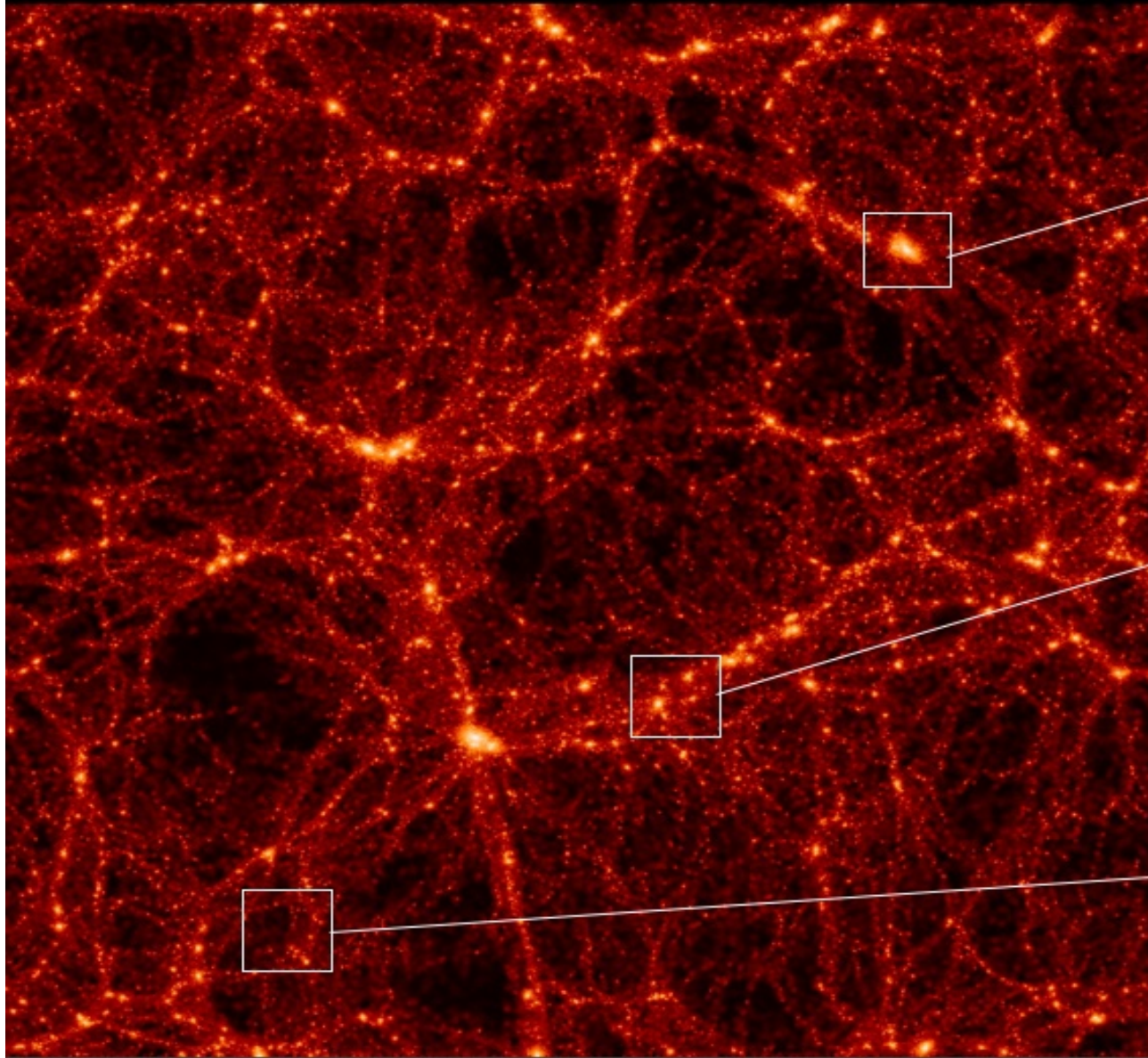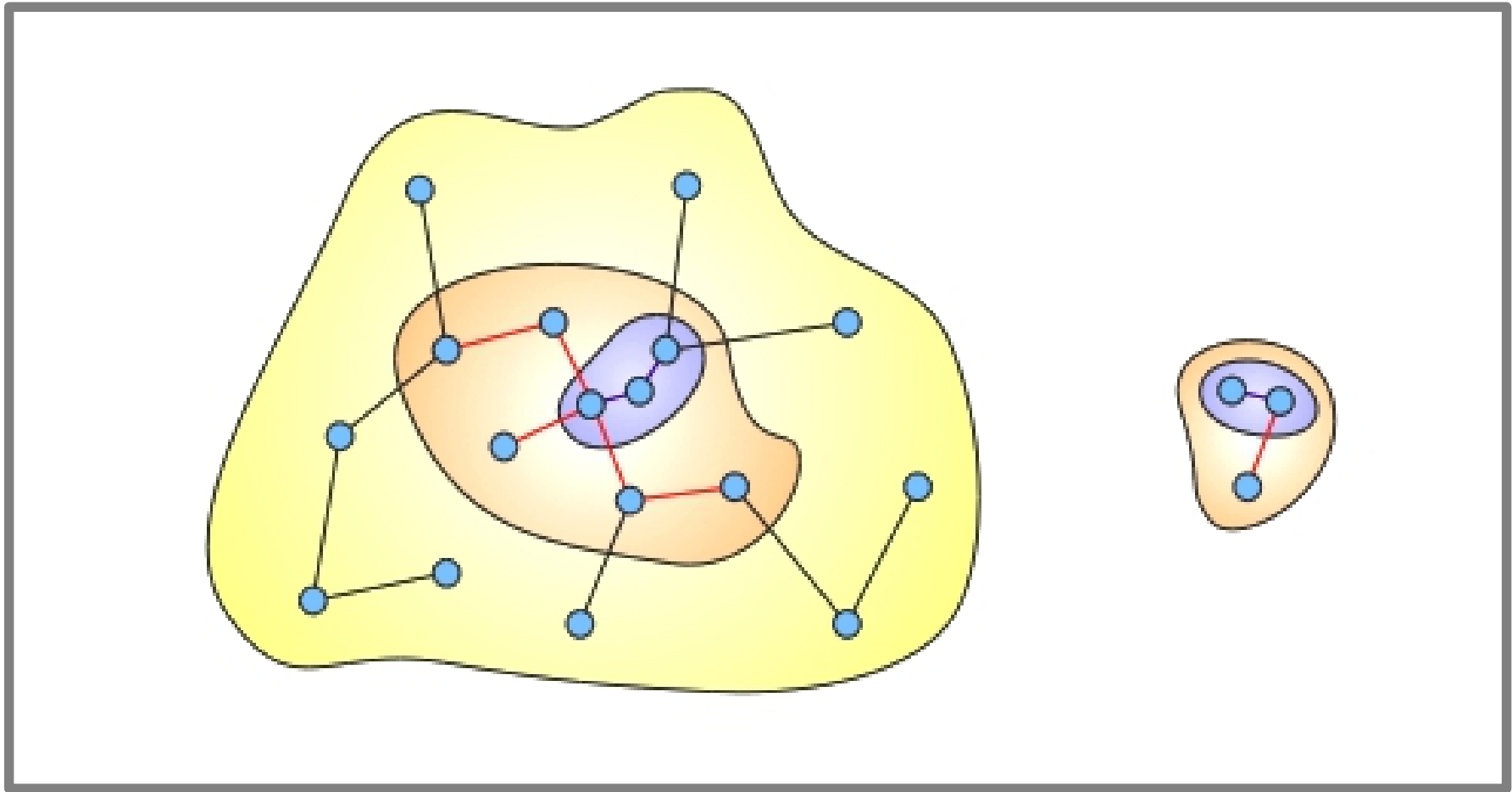
"Friends-of-friends" algorithm for identifying halos at fixed over-density compared to the mean inter-particle separation.

Navarro, Frenk & White 1996

$$\frac{\rho(r)}{\rho_{\mathrm{crit}}} = \frac{\delta_c}{(r/r_s)(1 + r/r_s)^2} \,, \qquad (3)$$

where $r_s = r_{200}/c$ is a characteristic radius and $\rho_{\mathrm{crit}} = 3H^2/8\pi G$ is the critical density (H is the current value of Hubble's constant); δ_c and c are two dimensionless parameters. Note that r_{200} determines the mass of the halo, $M_{200} = 200\rho_{\mathrm{crit}}(4\pi/3)r_{200}^3$, and that δ_c and c are linked by the requirement that the mean density within r_{200} should be $200 \times \rho_{\mathrm{crit}}$. That is,
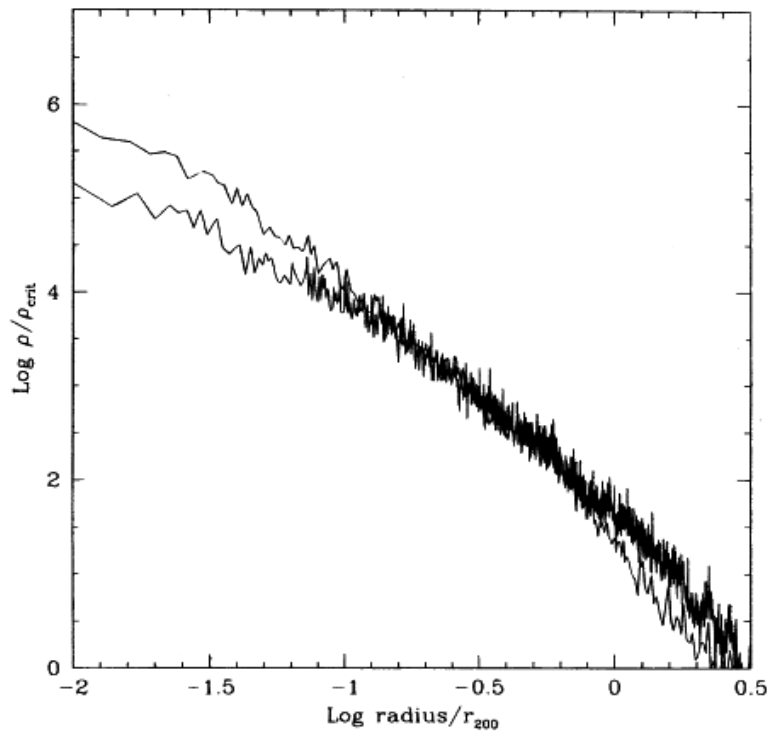
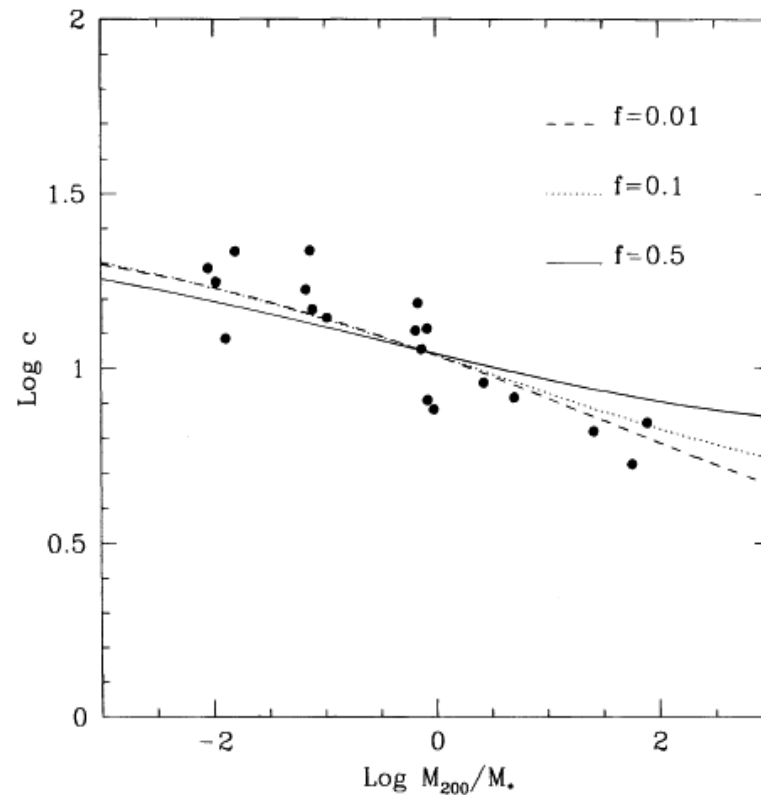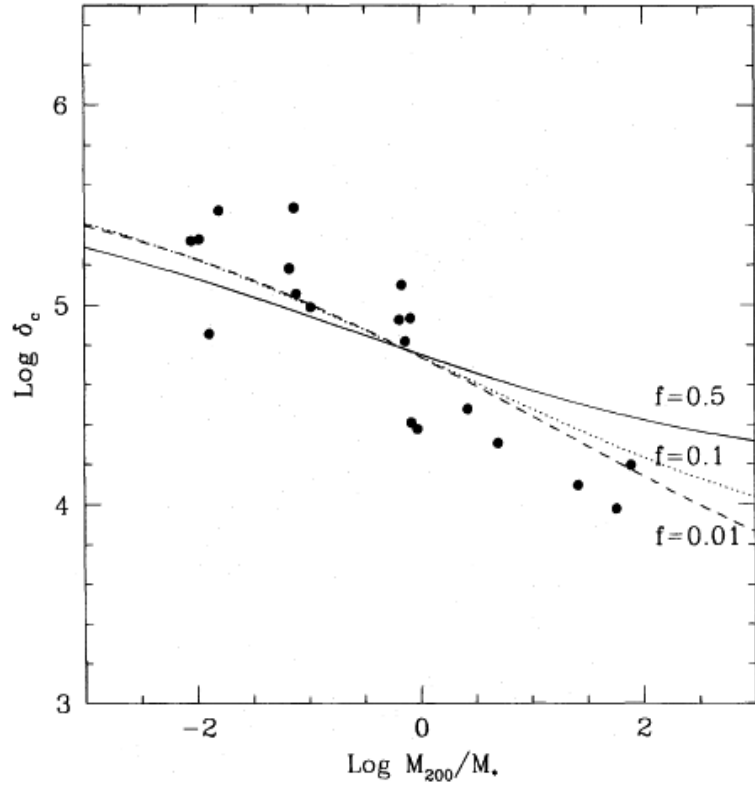$$\delta_c = \frac{200}{3} \frac{c^3}{[\ln(1 + c) - c/(1 + c)]}. \qquad (4)$$
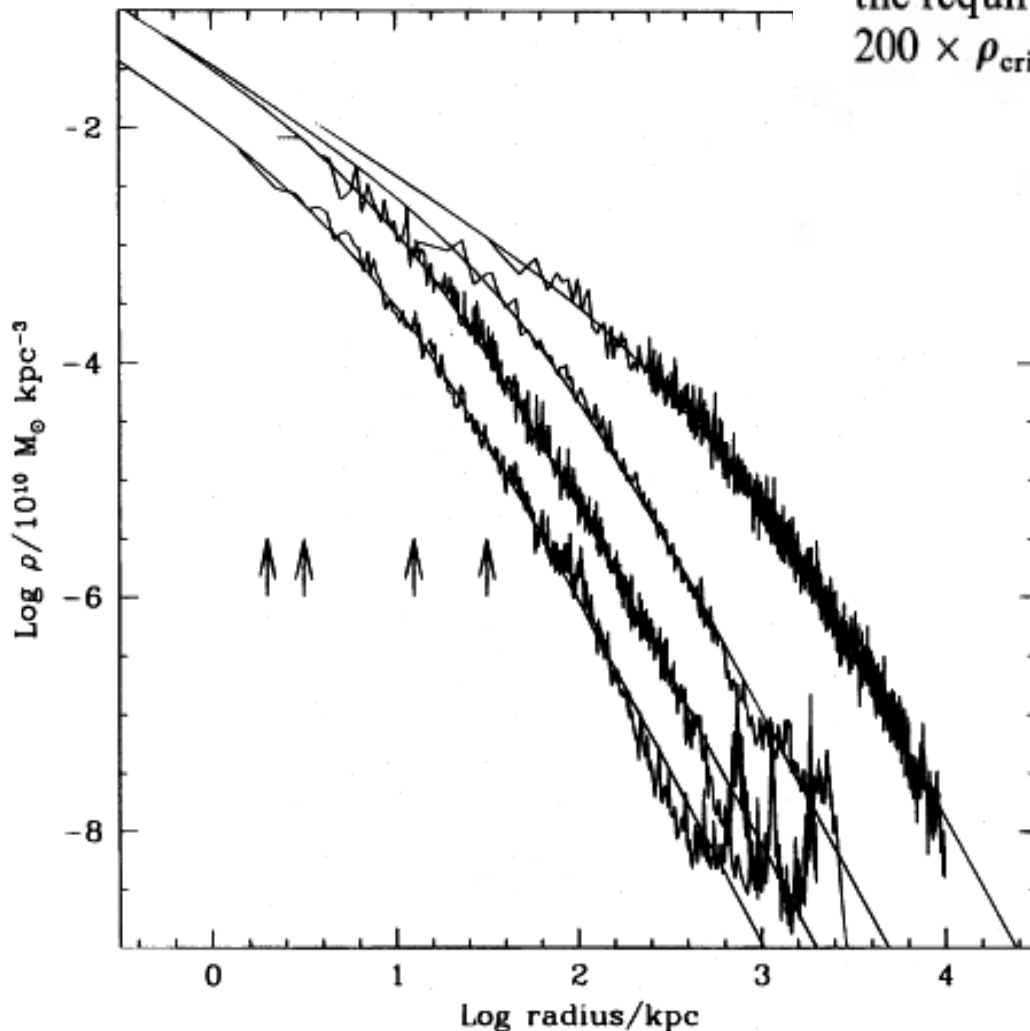
The Density Profiles of Dark Matter Halos Exhibit a "Universal" form
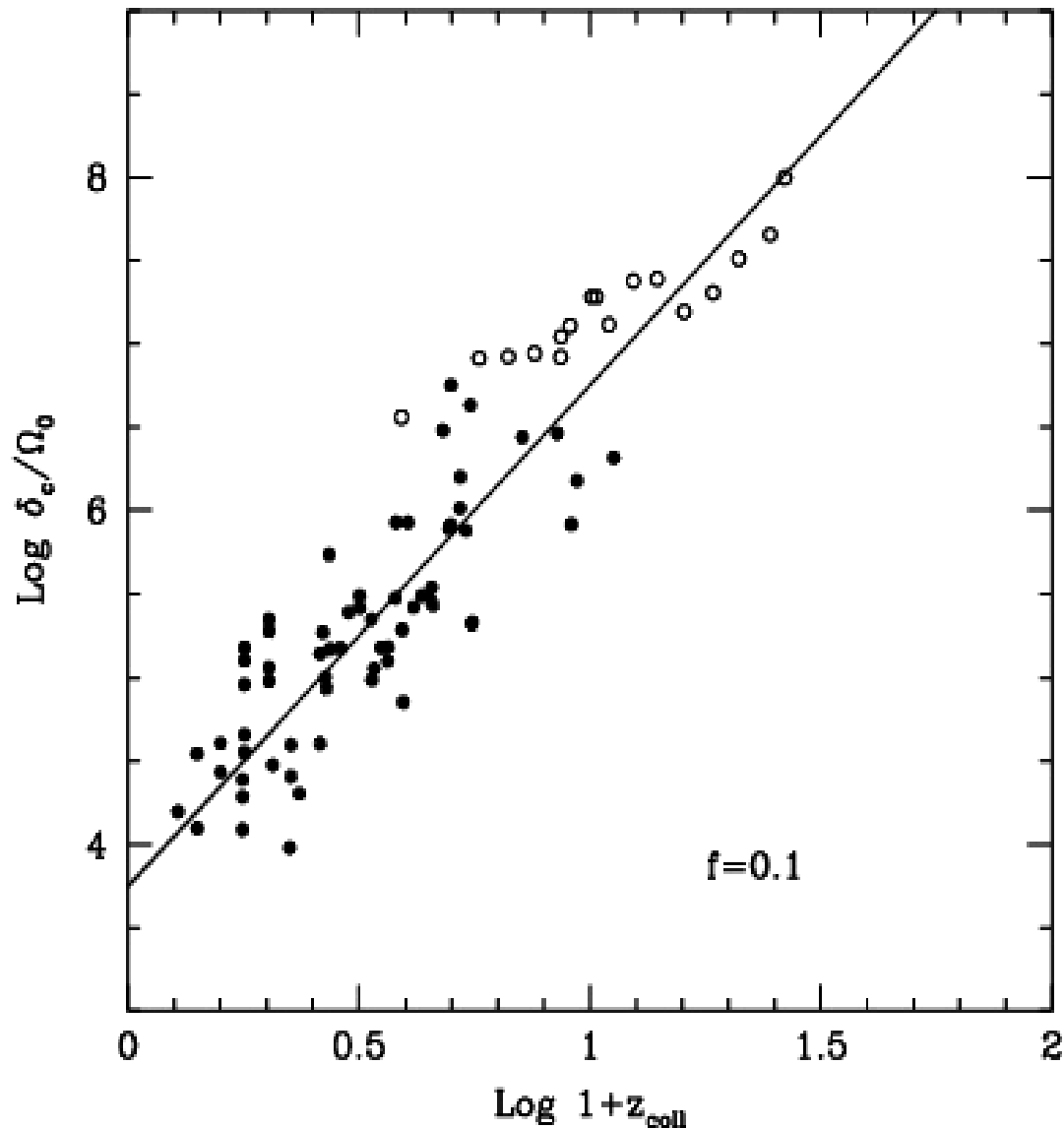
The same form fits for different cosmological parameters and power spectra of initial density perturbations.
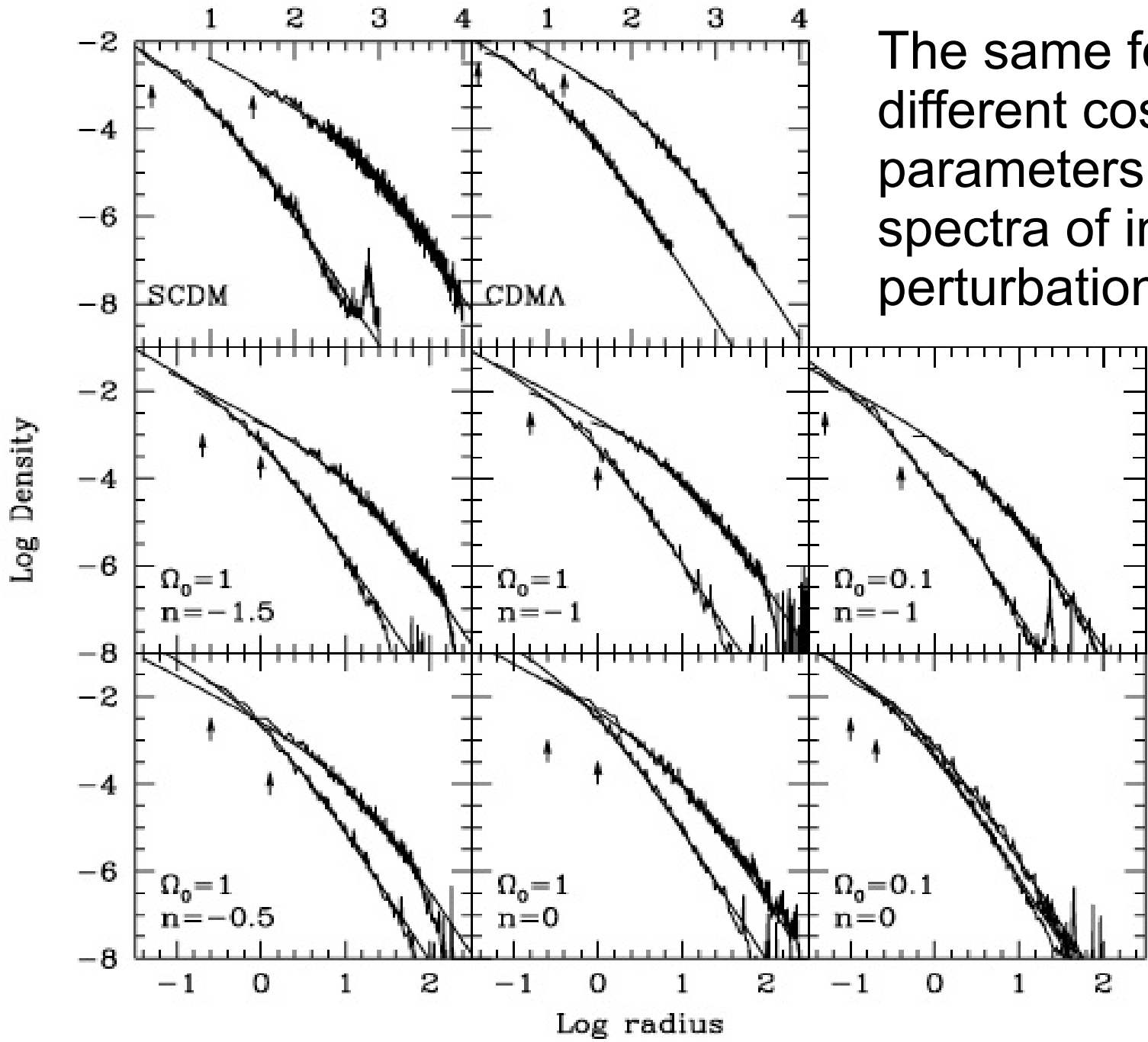
Less massive halos are more concentrated

Correlation between the characteristic density of the halo and the redshift at which a given fraction of its mass "collapsed" into a virialized structure.

Fig. 8.— The characteristic density of all halos in our series as a function of the redshift at which half of the final mass is in collapsed progenitors more massive than 10% of the final mass. Solid

Shapes of dark matter halos
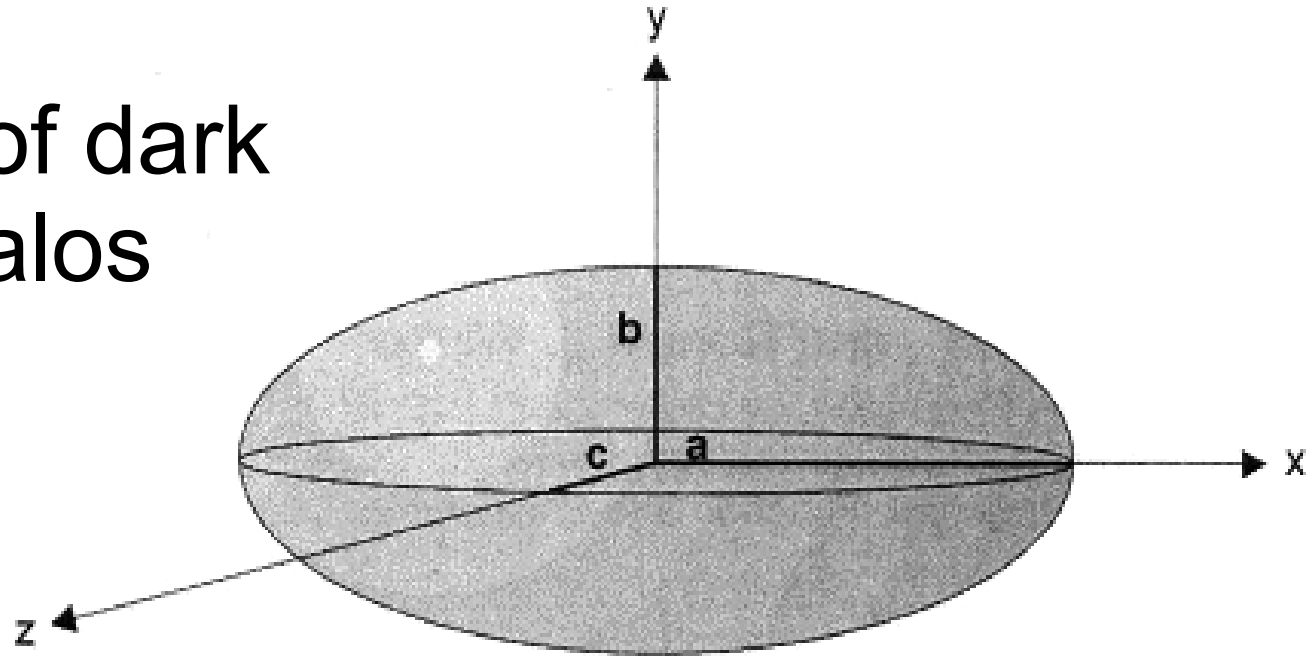
One way of quantifying the shape of a halo is to go one step beyond the spherical approximation and approximate halos by ellipsoids. Ellipsoids are characterised by three axes, a, b, c, with $a \geq b \geq c$, which are normally described in terms of ratios, $s \equiv c/a$, $q \equiv b/a$, and $p \equiv c/b$. Ellipsoids can also be described in terms of three classes, which have corresponding ratio ranges: prolate (sausage shaped) ellipsoids have $a > b \approx c$ leading to axial ratios of $s \approx q < p$, oblate (pancake shaped) ellipsoids have $a \approx b > c$ leading to axial ratios of $s \approx p < q$, and triaxial ellipsoids are in between prolate and oblate with $a > b > c$.

s=c/a (ratio of the shortest-to-longest axes) decreases at high halo masses and high redshifts
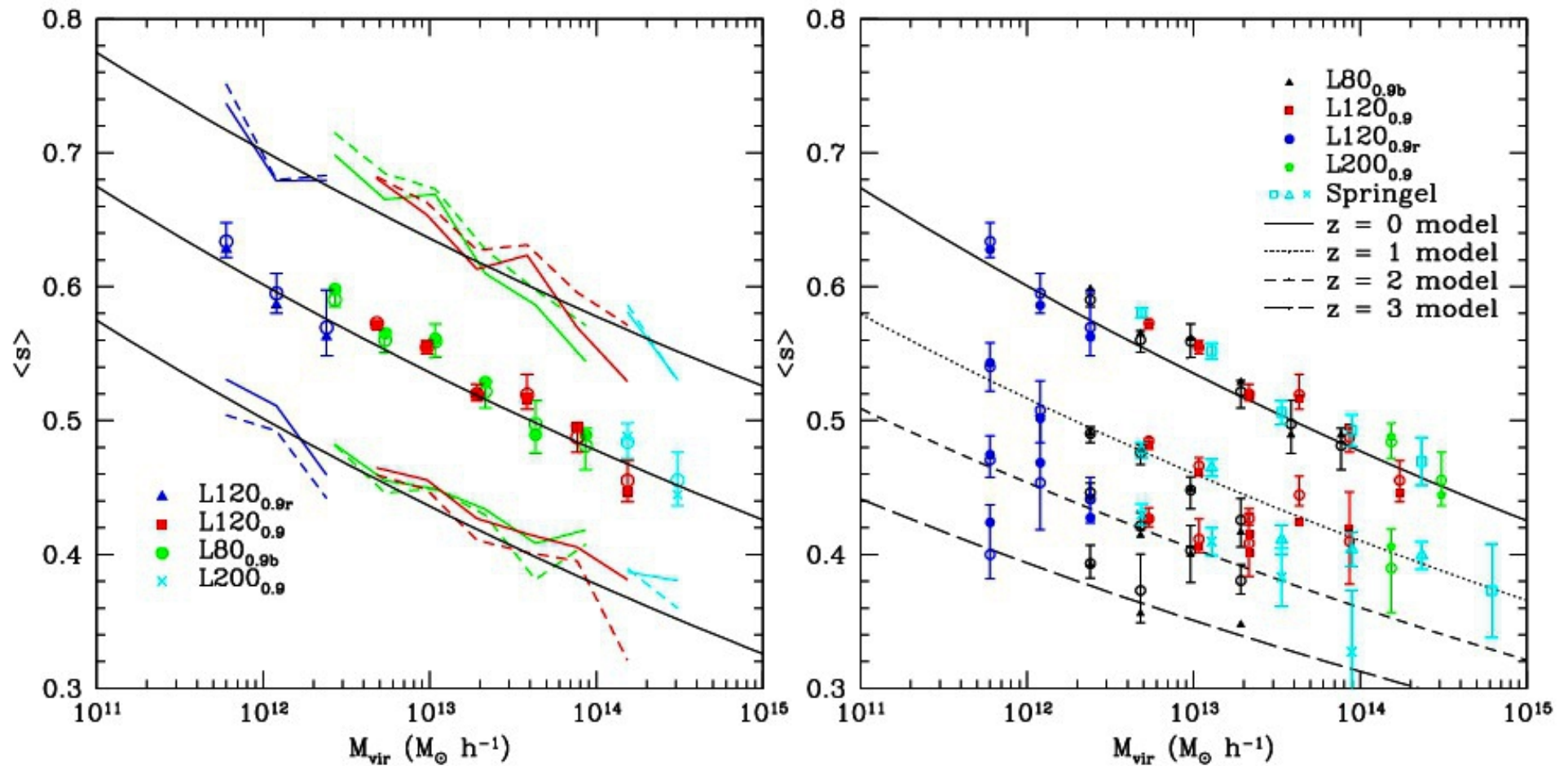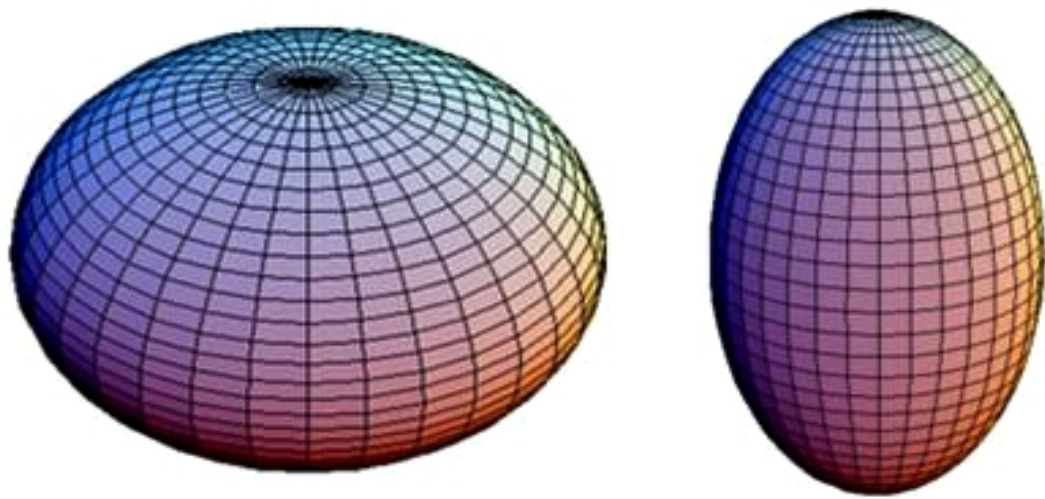
oblate spheroid   *prolate spheroid*

Often ellipsoids are described in terms of their triaxiality (prolate, oblate, or triaxial). One way of expressing the triaxiality of an ellipsoid is by using the triaxiality parameter Franx, Illingworth & de Zeeuw (1991):

$$T \equiv \frac{a^2 - b^2}{a^2 - c^2} = \frac{1 - q^2}{1 - s^2}. \tag{12}$$

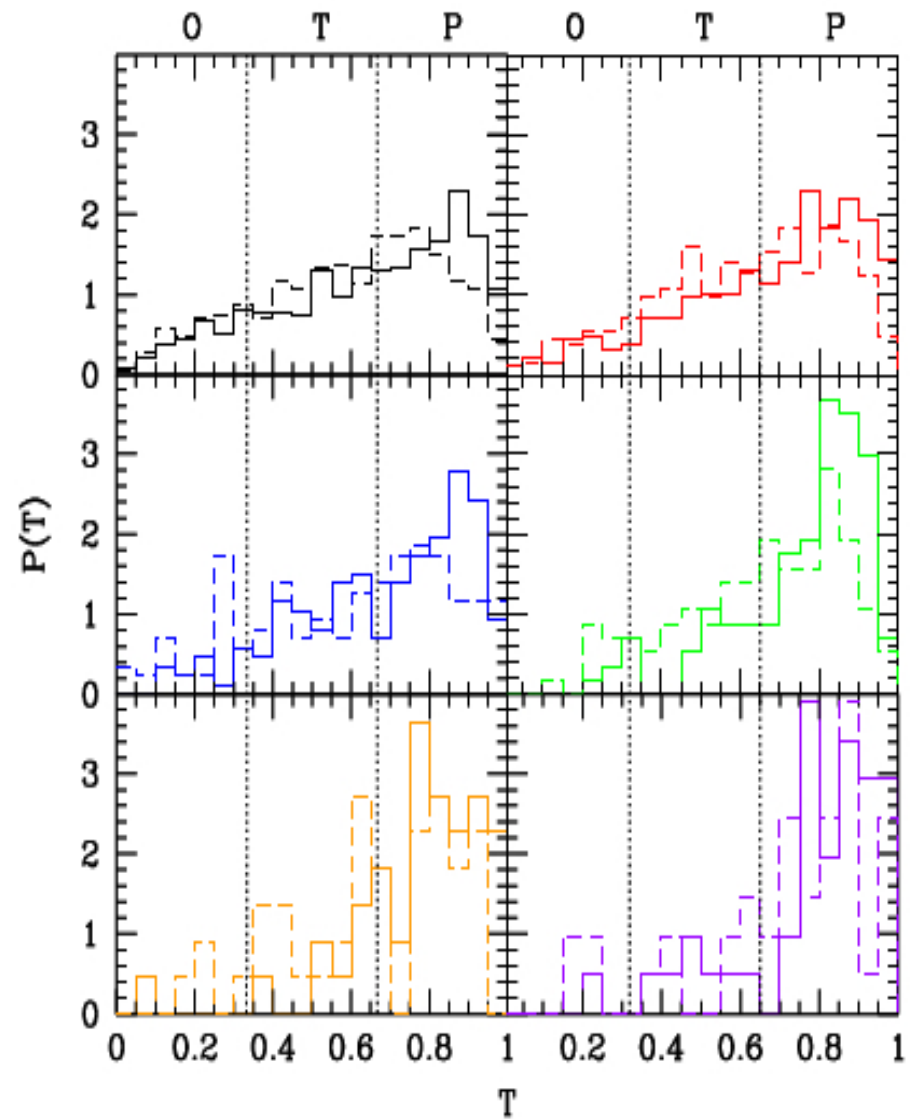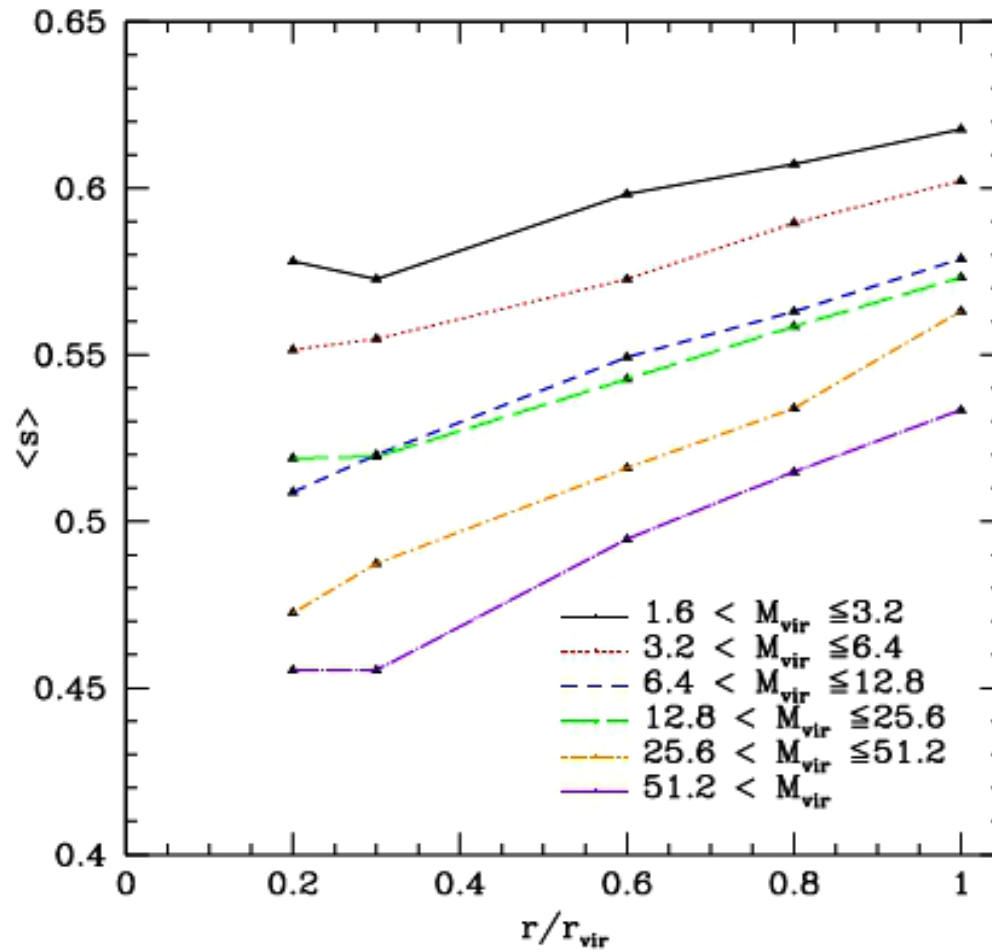An ellipsoid is considered *oblate* if $0 < T < 1/3$, *triaxial* with $1/3 < T < 2/3$, and *prolate* if $2/3 < T < 1$.

Figure 8. Triaxiality of halos at $z = 0$ at $R = 0.3R_{\mathrm{vir}}$ (solid) and R_{vir} (dashed). Beginning with the top left histogram and moving right, then down, the triaxiality of halos is divided in to the same mass bins as in Figure 7.

Halos are rounder on the outside than on the inside

ANGULAR MOMENTUM OF HALOS AS CHARACTERIZED BY SPIN

The spin parameter of a halo is a dimensionless quantity introduced by Peebles (1969) that indicates the amount of ordered rotation compared to the internal random motions. For a halo of mass M and angular momentum J it is defined as

$$\lambda = \frac{|J|\,|E|^{1/2}}{GM^{5/2}}, \tag{3}$$

where the total energy $E = T + U$ with T the kinetic energy of the halo after subtracting its bulk motion and U the potential energy of the halo produced by its own mass distribution.

The specific angular momentum j and kinetic e T of each halo containing N_p particles are given by:

$$j \;=\; \frac{1}{N_\mathrm{p}} \sum_{i=1}^{N_\mathrm{p}} r_i \times v_i$$

$$T \;=\; \frac{1}{2} M_\mathrm{h} \sum_{i=1}^{N_\mathrm{p}} v_i^2$$

where r_i is the position vector of particle i relative to the halo centre, and v_i is its velocity relative to the halo centre of momentum.
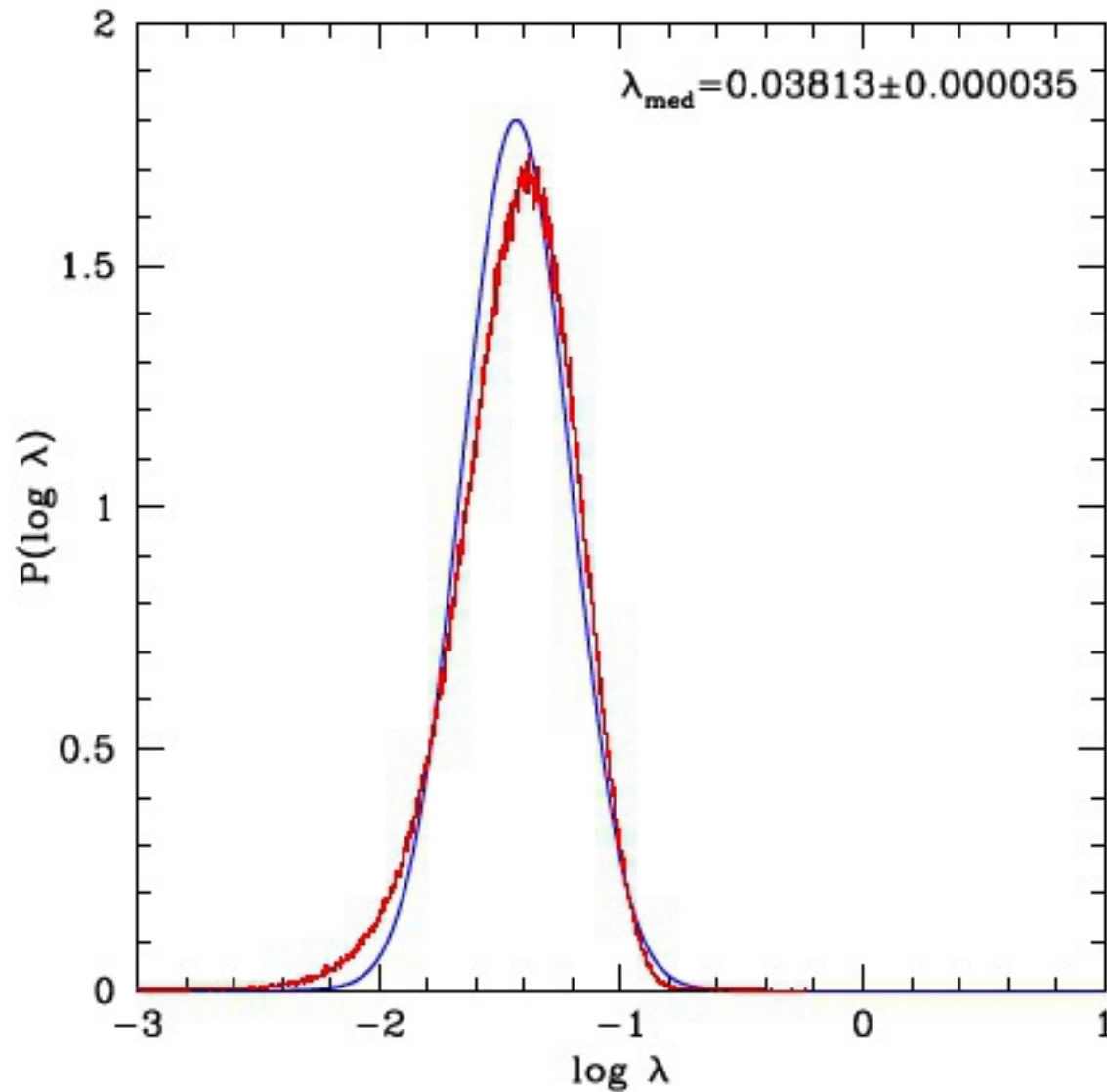
The halo potential energy, U, is calculated using all halo particles if $M_\mathrm{h} \leqslant 1000 m_\mathrm{p}$, and is rescaled up from that of 1000 randomly-sampled particles otherwise. The potential is that used in the simulation itself:

$$U = \left(\frac{N_\mathrm{p}^2 - N_\mathrm{p}}{N_\mathrm{sel}^2 - N_\mathrm{sel}} \right) \left(\frac{-G m_\mathrm{p}^2}{\eta} \right) \sum_{i=1}^{N_\mathrm{sel}-1} \sum_{j=i+1}^{N_\mathrm{sel}} -W_2(r_{ij}/\eta)$$

where N_sel is the number of selected particles ($N_\mathrm{sel} \leqslant 1000$), η is the softening length (see Table 1), r_{ij} is the magnitude of the separation vector between the ith and jth particles in the halo, and the softening kernel (see Springel et al. 2001) is:

$$W_2(u) = \begin{cases} \frac{16}{3}u^2 - \frac{48}{5}u^4 + \frac{32}{5}u^5 - \frac{14}{5}, & 0 \leqslant u \leqslant \frac{1}{2}, \\ \frac{1}{15u} + \frac{32}{3}u^2 - 16u^3 + \frac{48}{5}u^4 \\ \quad - \frac{32}{15}u^5 - \frac{16}{5}, & \frac{1}{2} \leqslant u \leqslant 1, \\ -\frac{1}{u}, & u \geqslant 1 \end{cases}$$
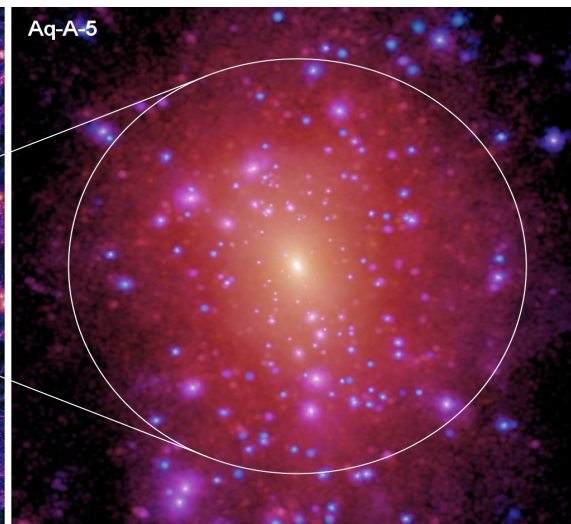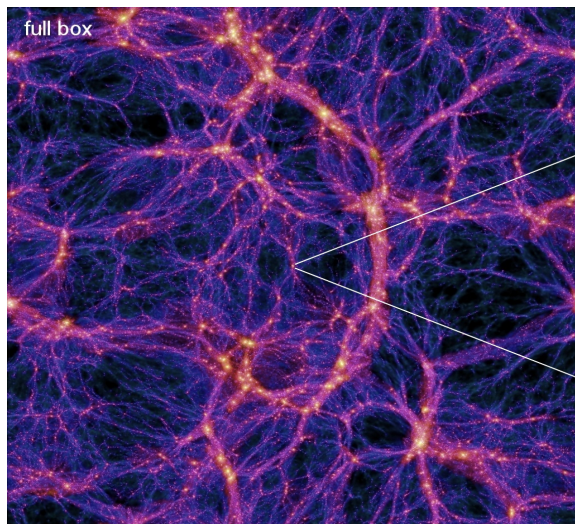
$$P(\log \lambda) = \frac{1}{\sigma_{\lg} \sqrt{2\pi}} \exp \left[-\frac{\log^2 (\lambda/\lambda_0)}{2\sigma_{\lg}^2} \right]$$


$\lambda_{med} = 0.03813 \pm 0.000035$

Substructure in Dark Matter Halos
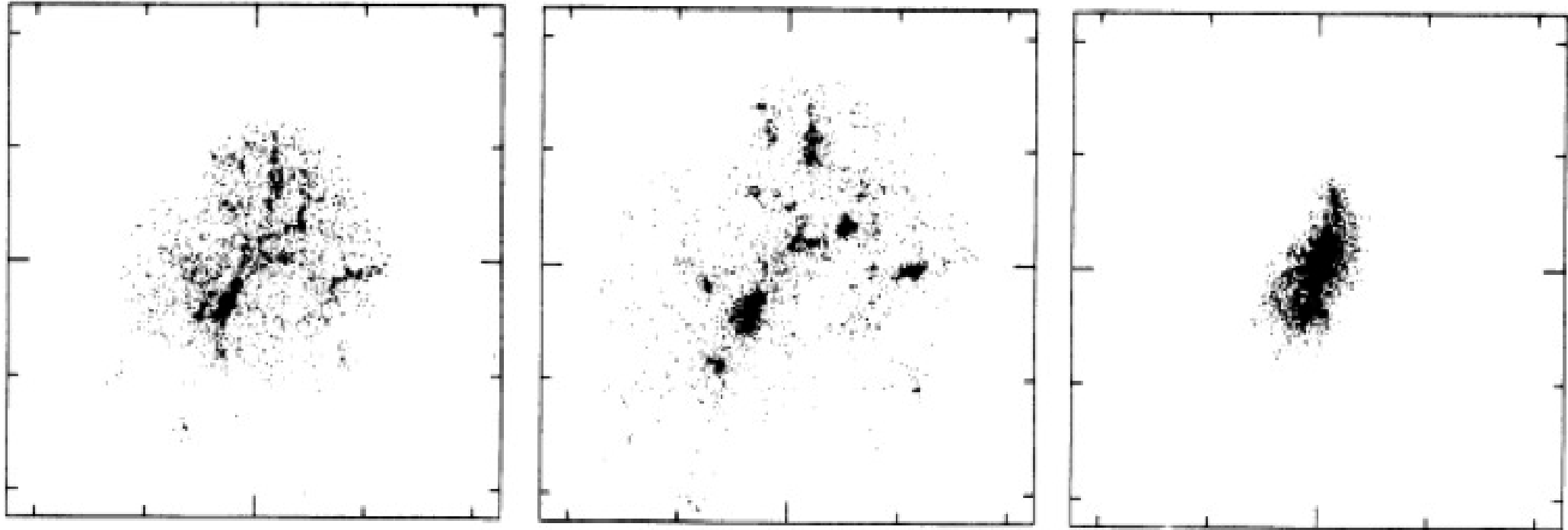
Early halos in simulations exhibited very little substructure – this was known as the "overnerging problem", because bound , virialized systems of multiple galaxies do exist (galaxy groups and clusters).

As computers became more powerful, simulations of every increasing particle number could be carried out. The higher resolution simulations revealed a rich hierarchy of substructure in dark matter halos.
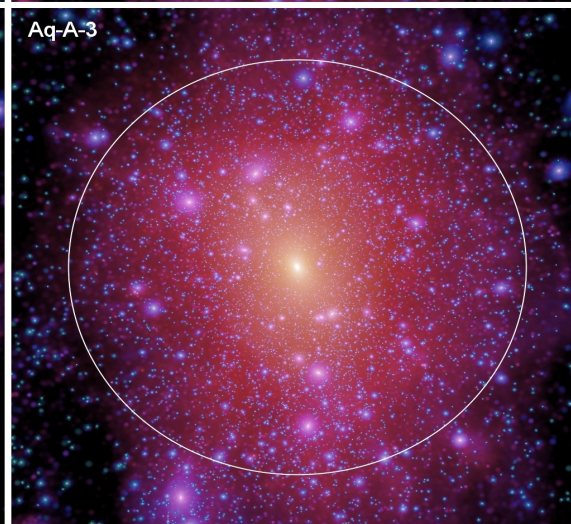
Aquarius simulations contains six examples of an isolated halo similar in mass to that of the Milky Way. These are simulated in their full cosmological context (assuming the concordance LCDM cosmology) and at various resolutions up to about 200 million particles (counted within the radius where the enclosed density is 200 times the cosmic mean). One halo is also simulated at even higher resolution, resulting in almost 1.5 billion particles within this radius.
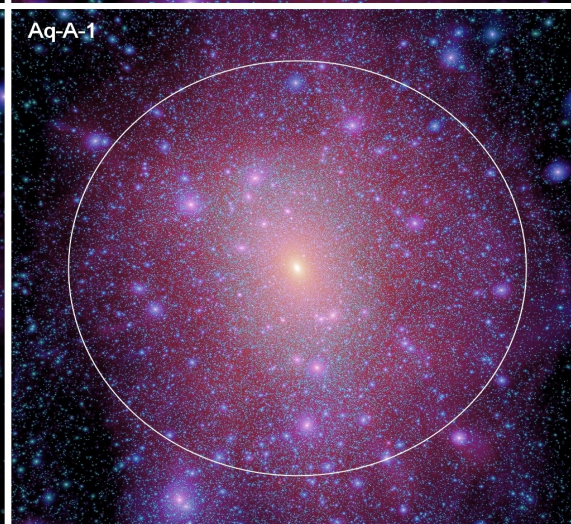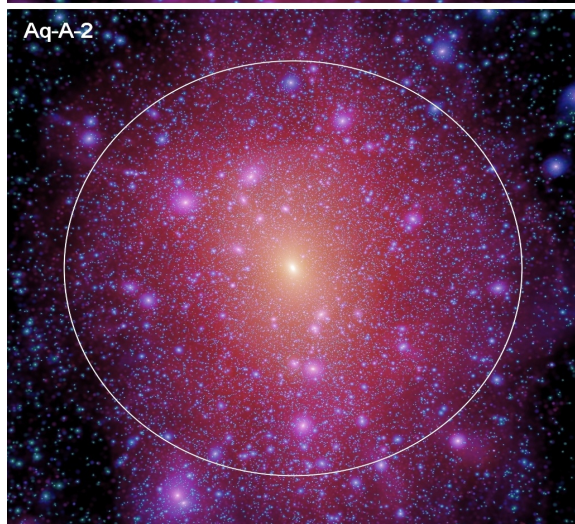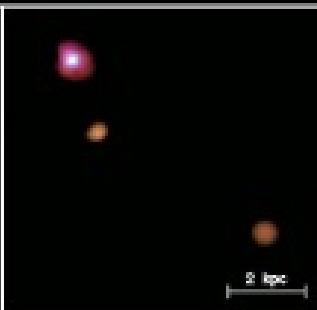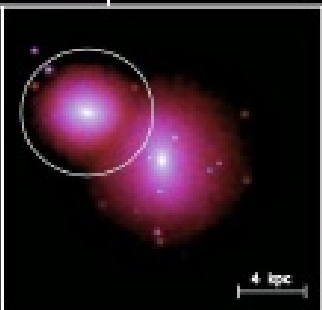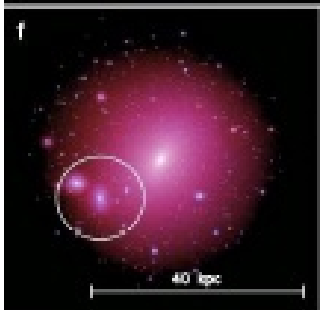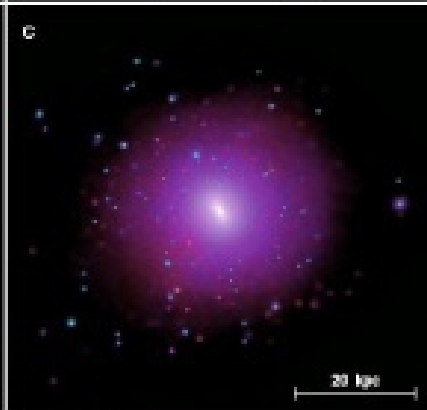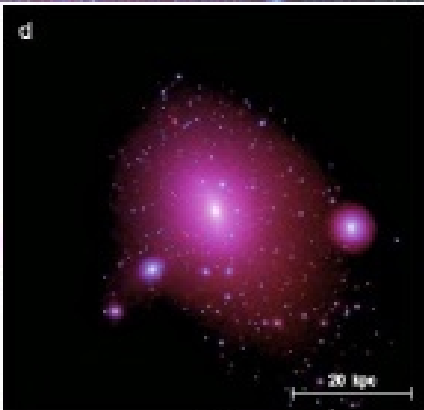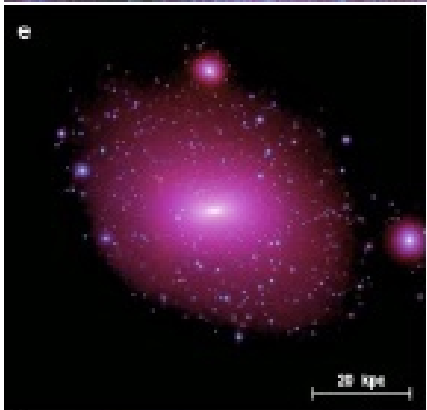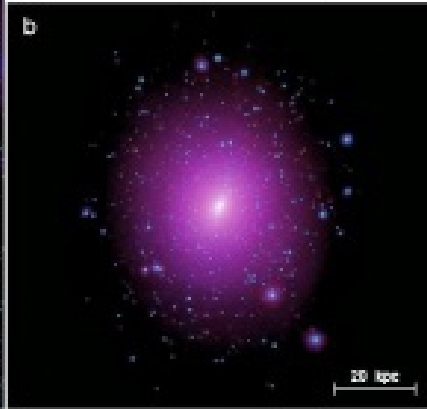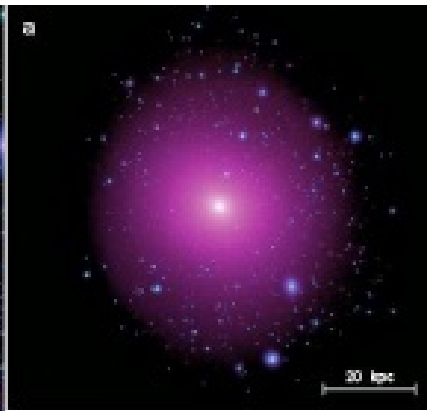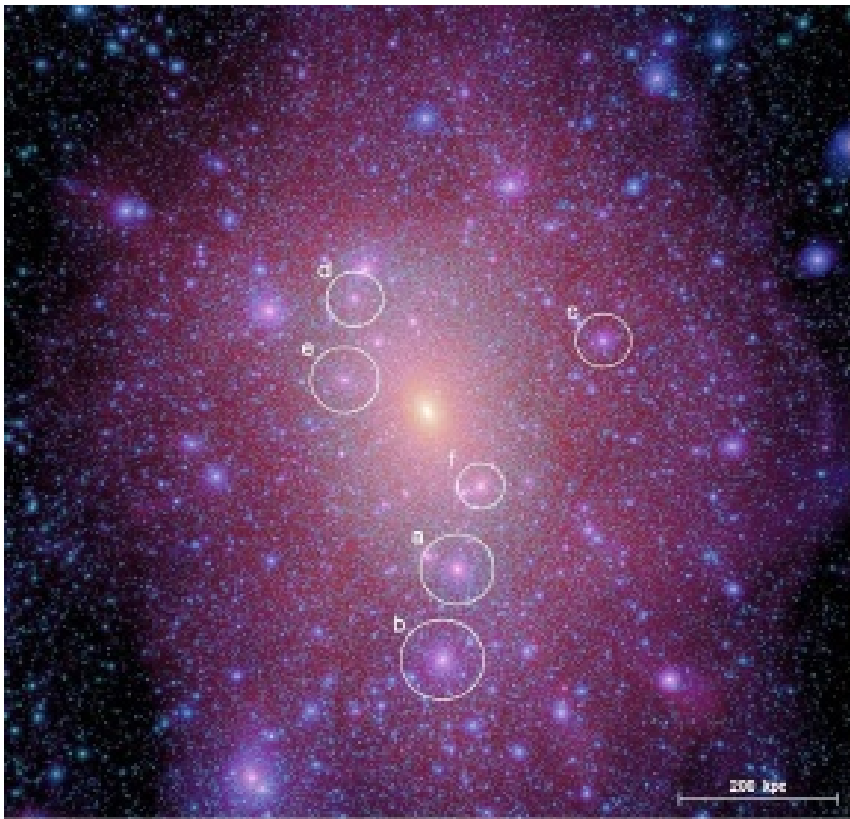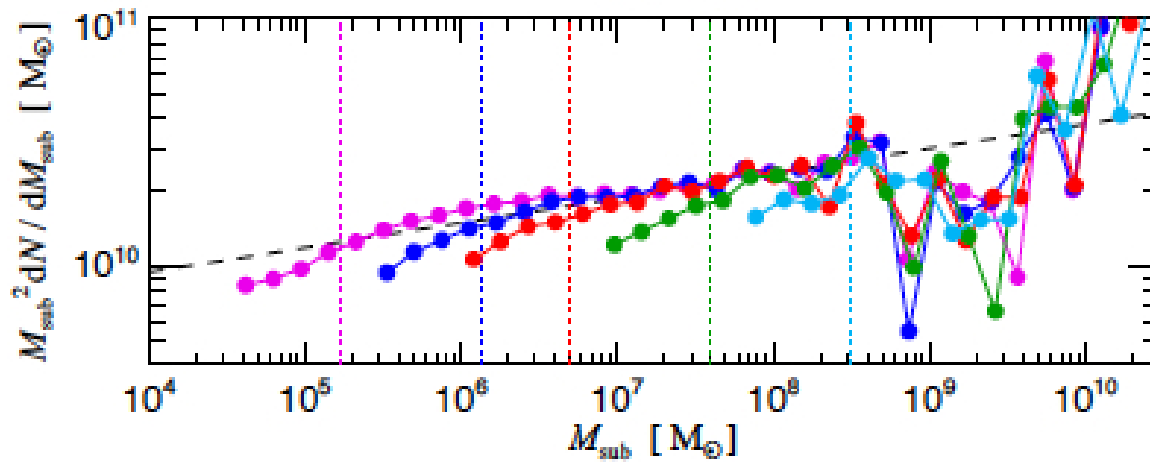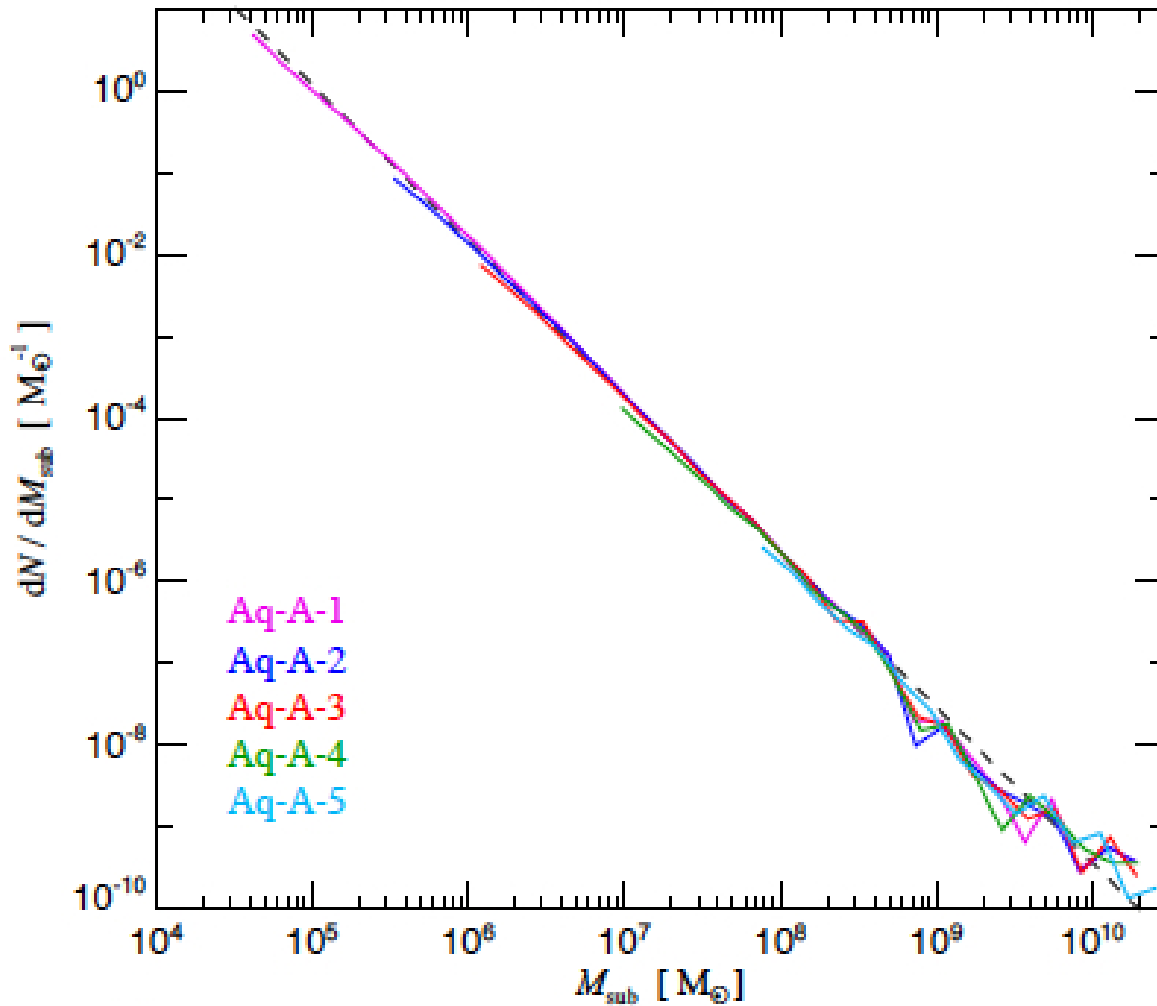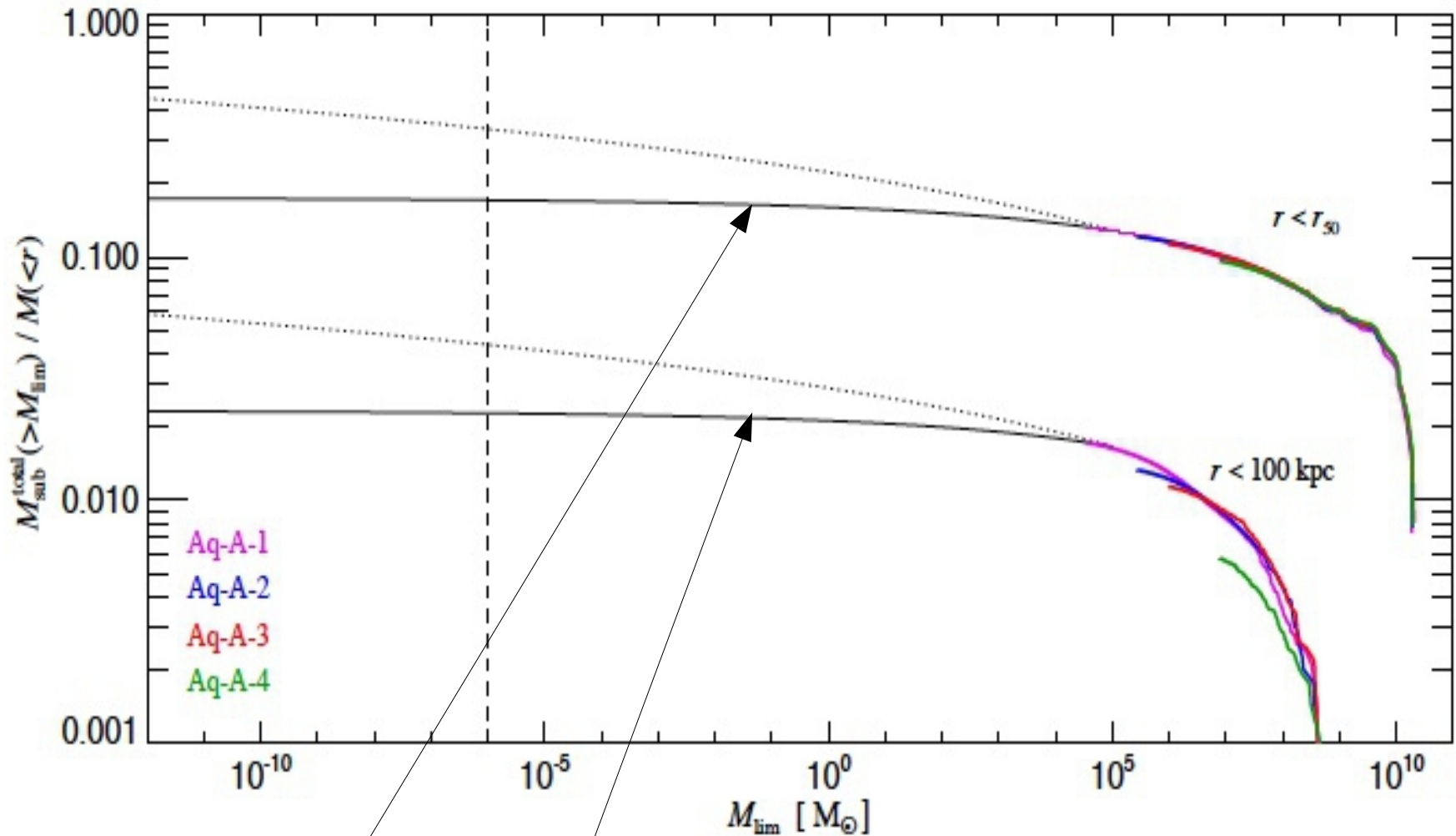
In the highest resolution simulation, one even finds "substructures within substructures"
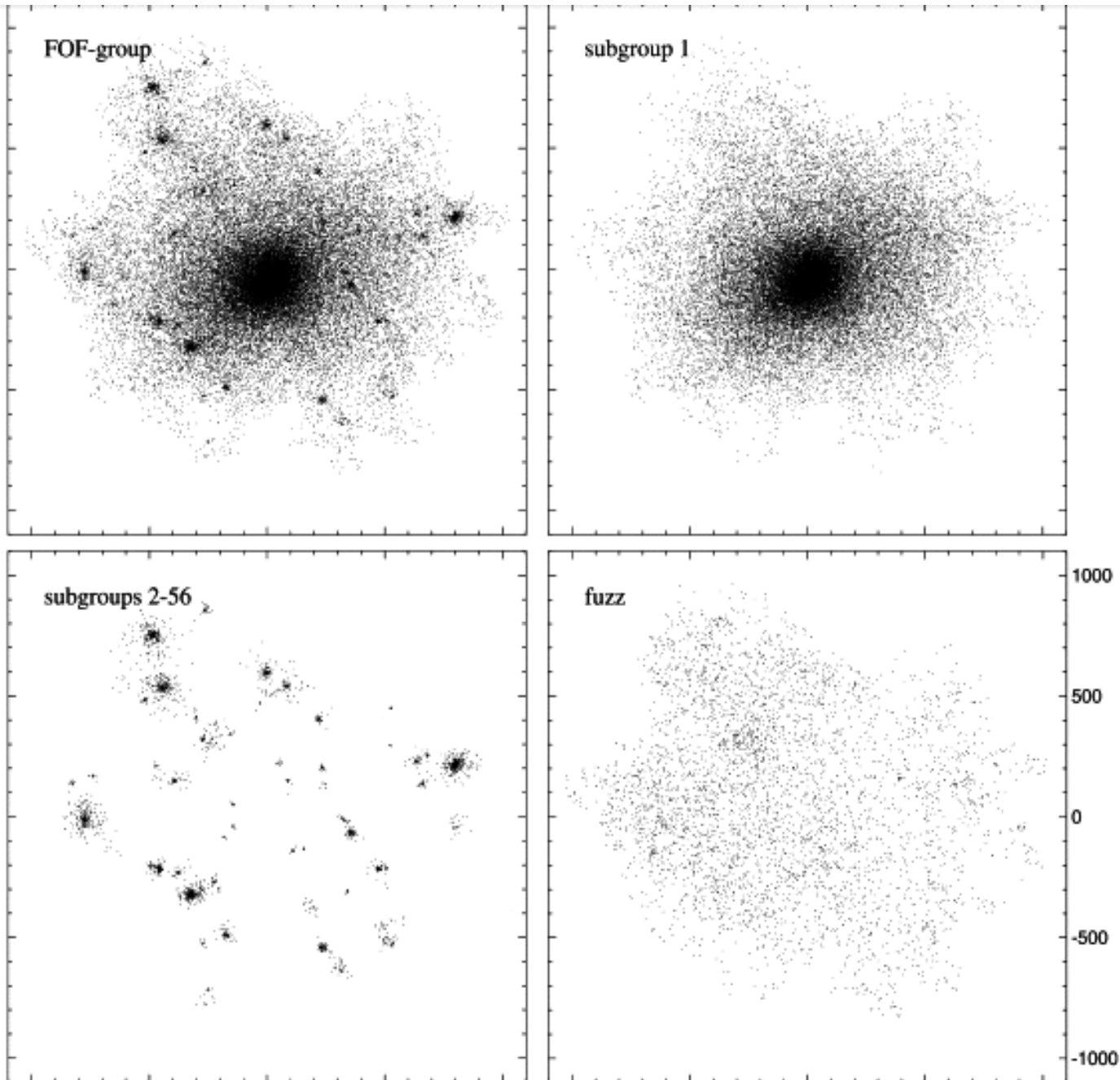
Sub-halo identification algorithms, eg. SUBFIND (Springel et al 2001) employ a variable link-length/density threshold to identify local density maxima on top of the global one.

Subhalo mass function is a power law with slope -1.9

Substructure mass function extrapolated using -1.9 power law: less than 0.2 with the half-mass radius
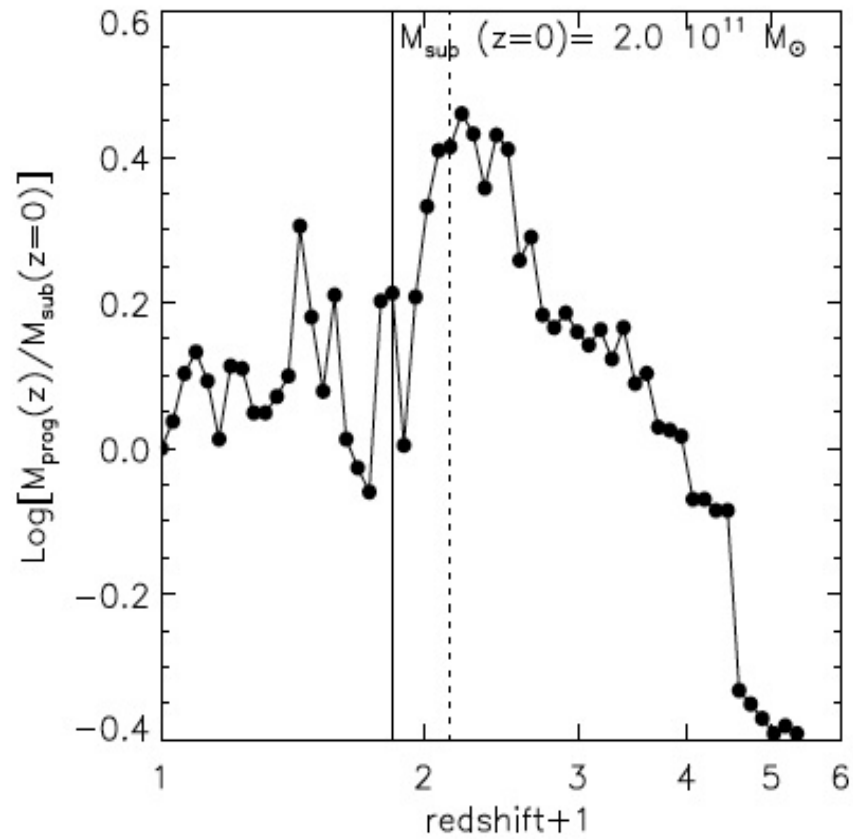
Figure 9. Example for a typical mass accretion history for a sub-halo of mass $2 \times 10^{11} h^{-1} M_\odot$ (lower panel), and the corresponding variation of mass for the parent halo in which the subhalo resides (top panel). The vertical solid line corresponds to the last time the subhalo is outside the main progenitor of the cluster; the dotted line corresponds to the time the subhalo becomes a substructure
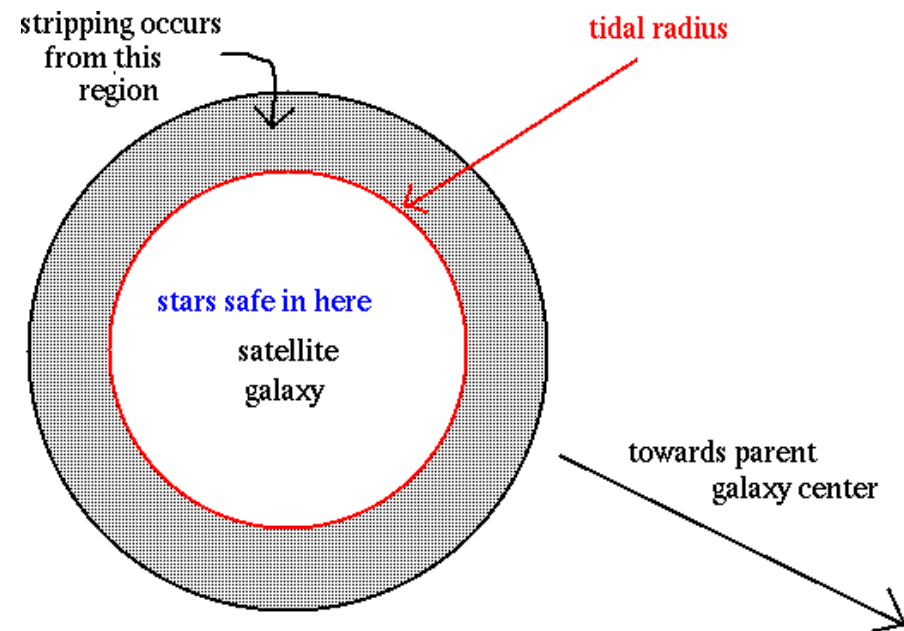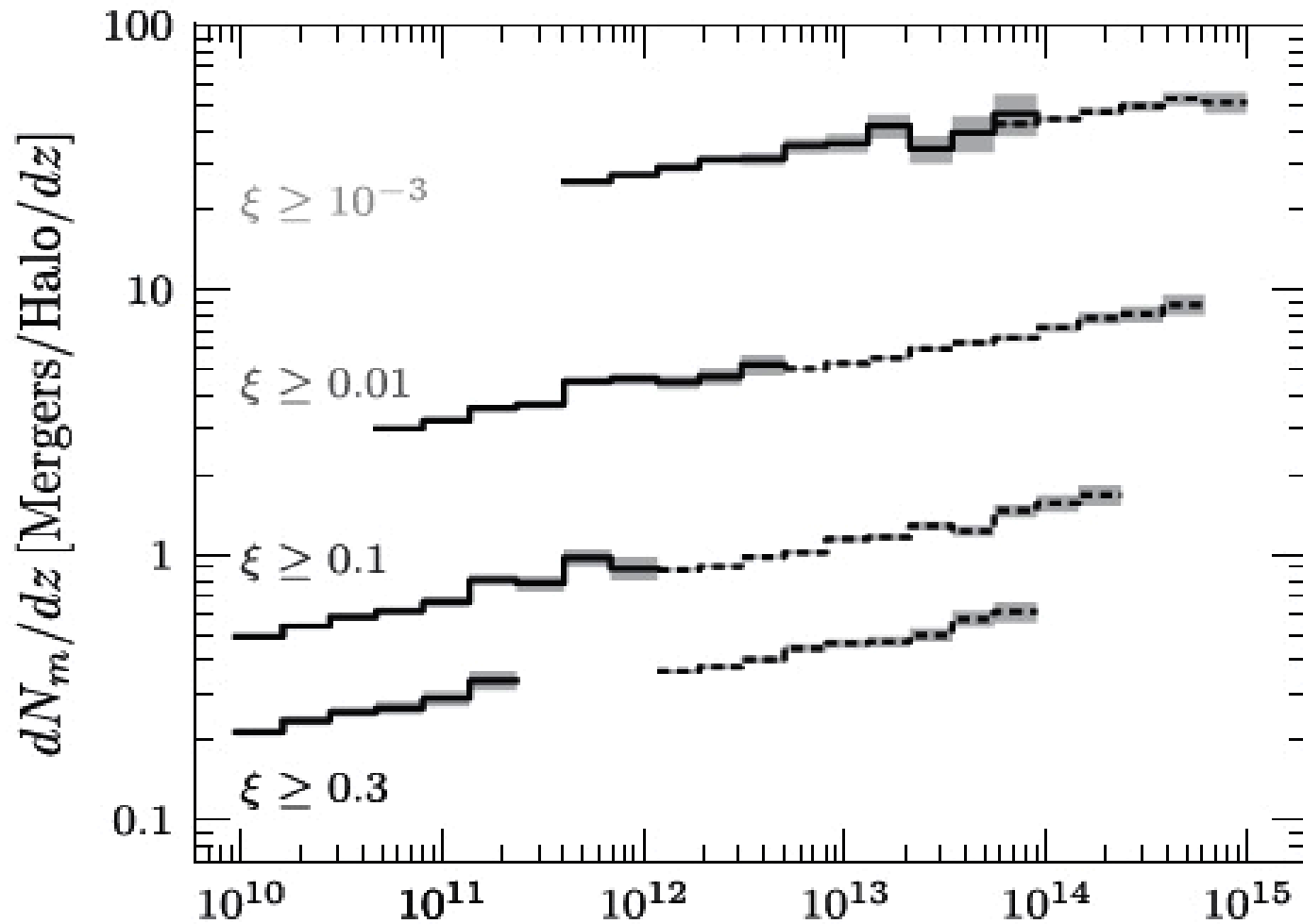
Merger histories of dark matter halos
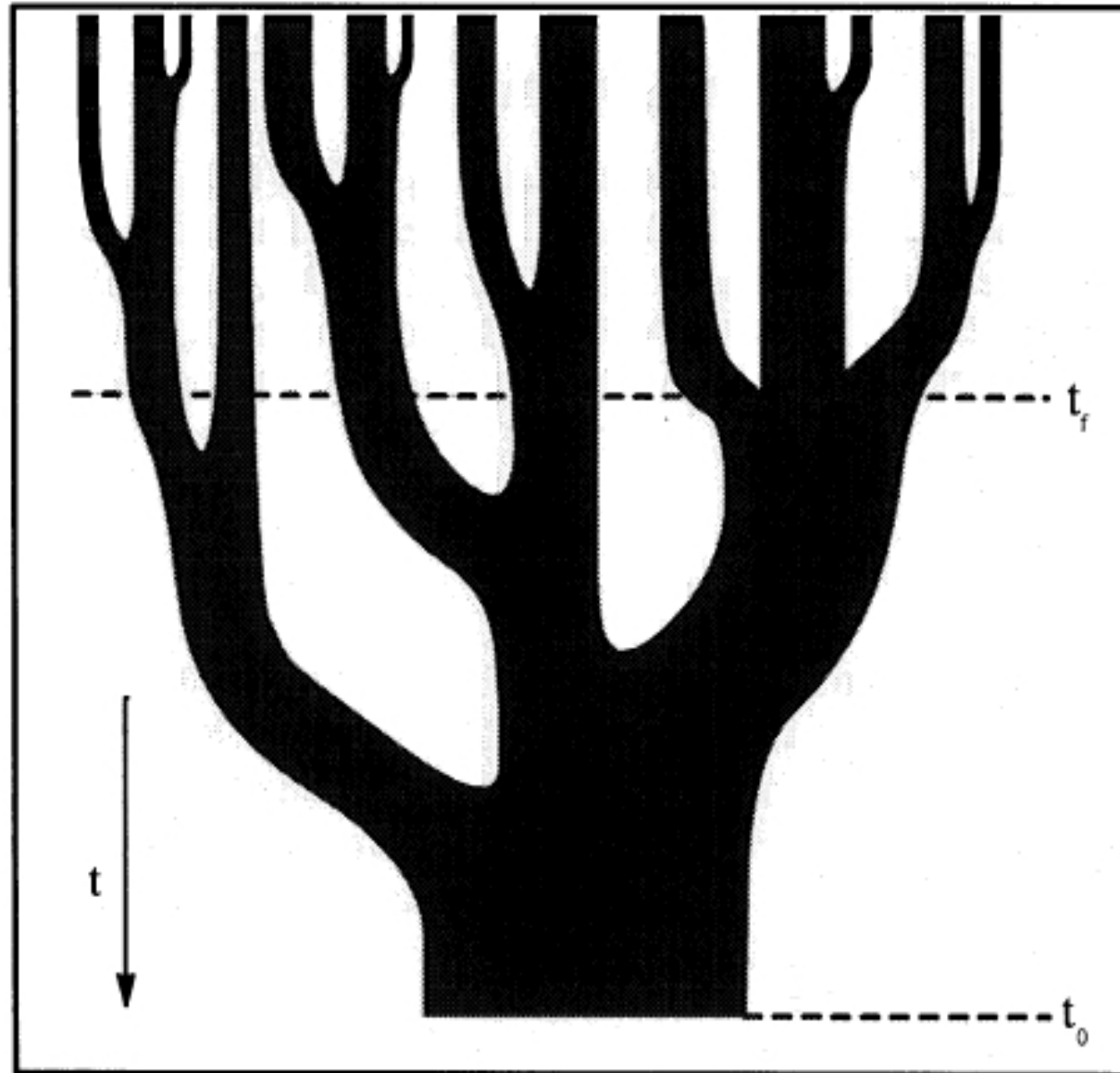
Number of mergers undergone by halos in the Millennium I and II simulations over history as a function of mass ratio M_i/M_1
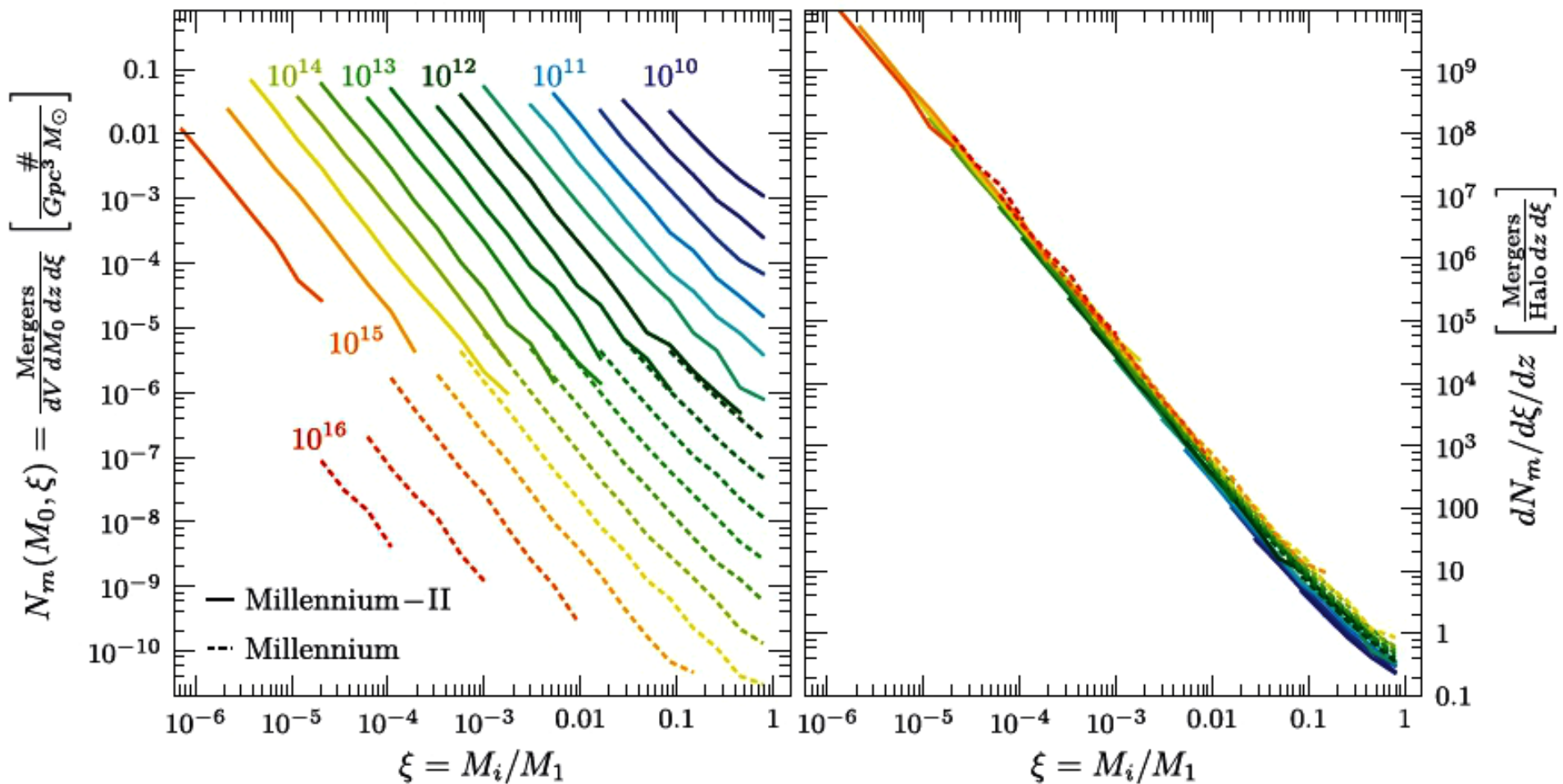
Results arranged in bins of halo mass

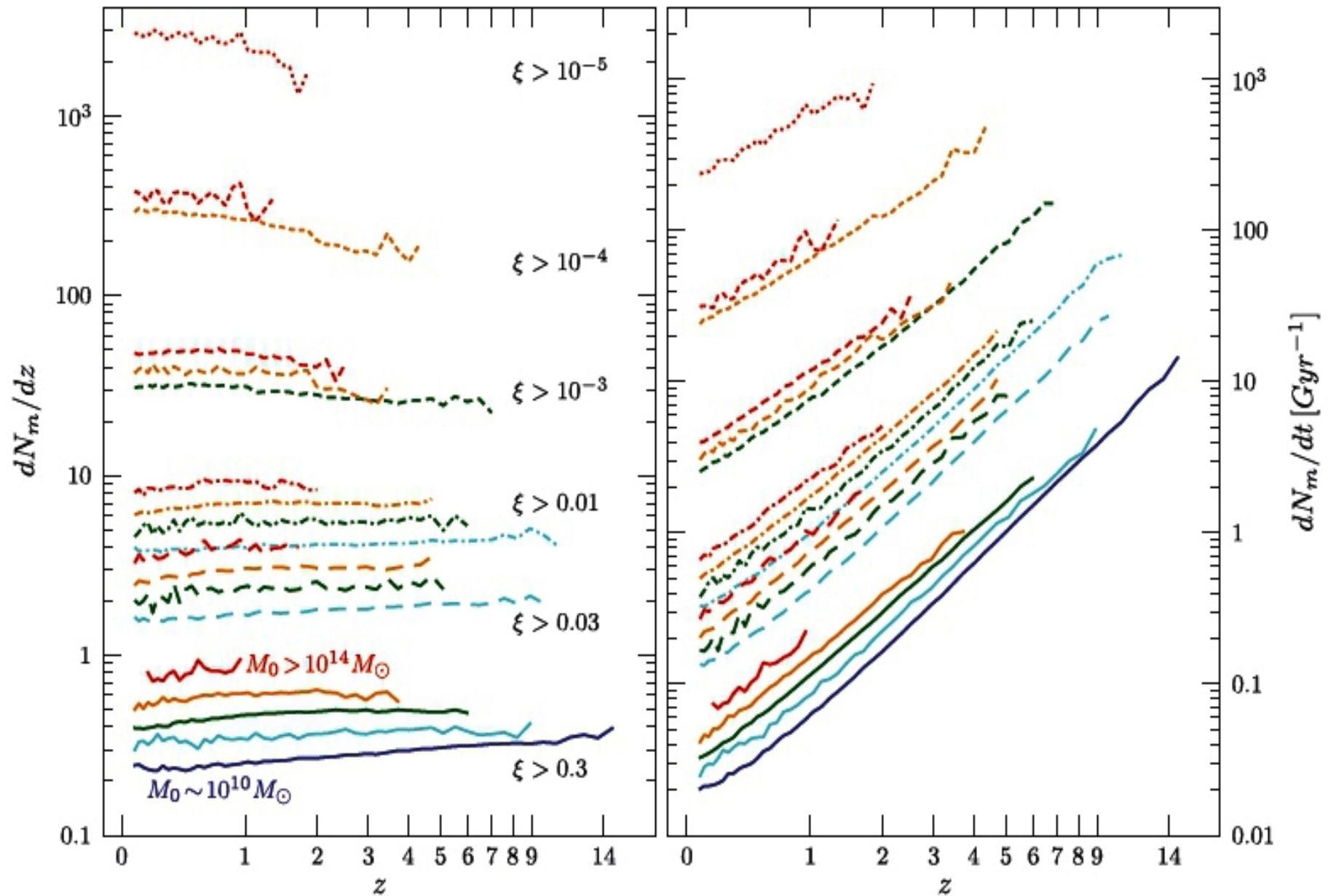Scaled by the number of halos in the simulation at the the present day.

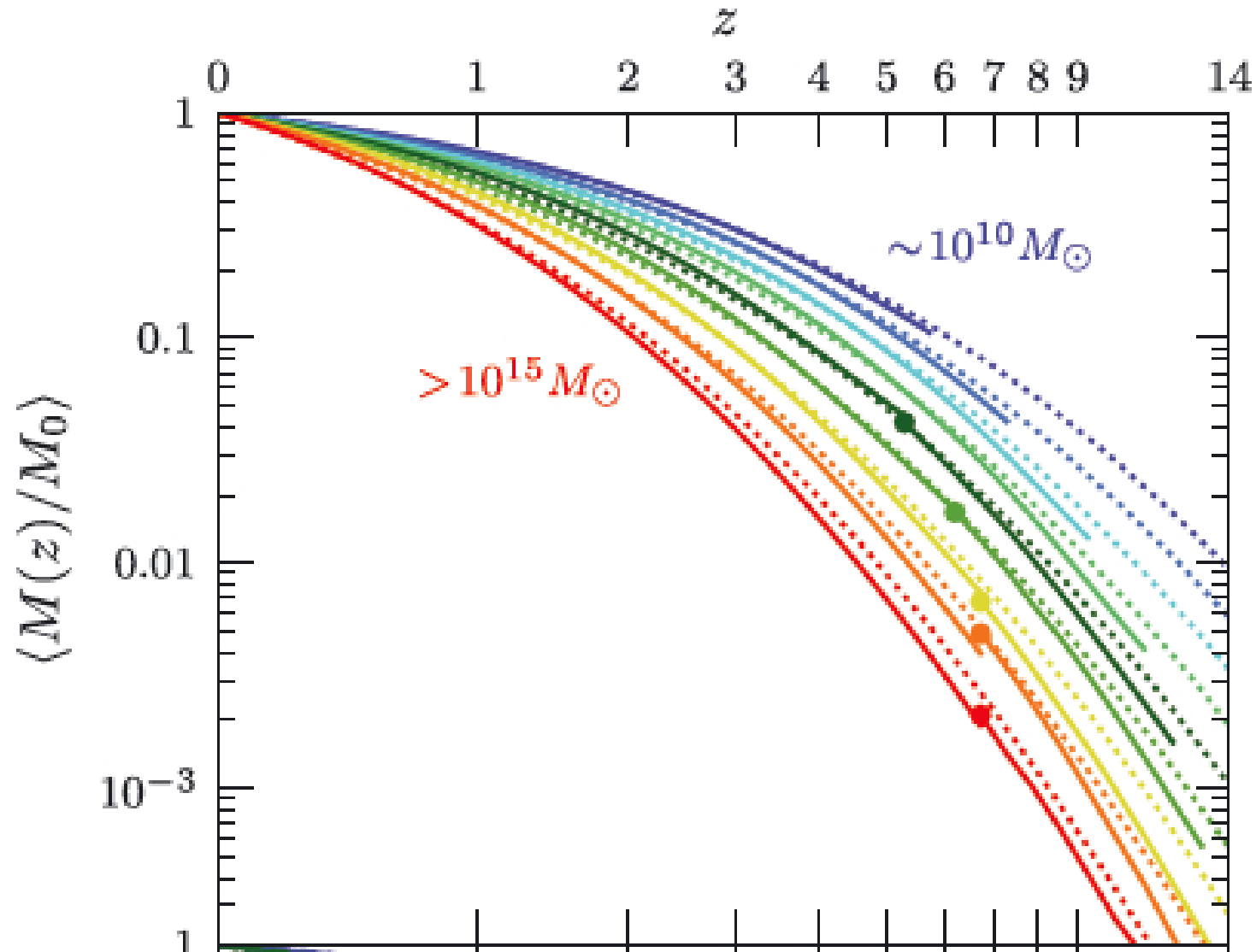# Halo mass dependence of the merging rate is very weak.

$$\frac{dN_m}{d\xi dz}(M, \xi, z) = A \left(\frac{M}{10^{12}\,M_\odot}\right)^\alpha \xi^\beta \exp\left[\left(\frac{\xi}{\tilde{\xi}}\right)^\gamma\right](1+z)^\eta.$$

We find the best-fitting parameters to be $(\alpha, \beta, \gamma, \eta) = (0.133, -1.995, 0.263, 0.0993)$ and $(A, \tilde{\xi}) = (0.0104, 9.72 \times 10^{-3})$. The

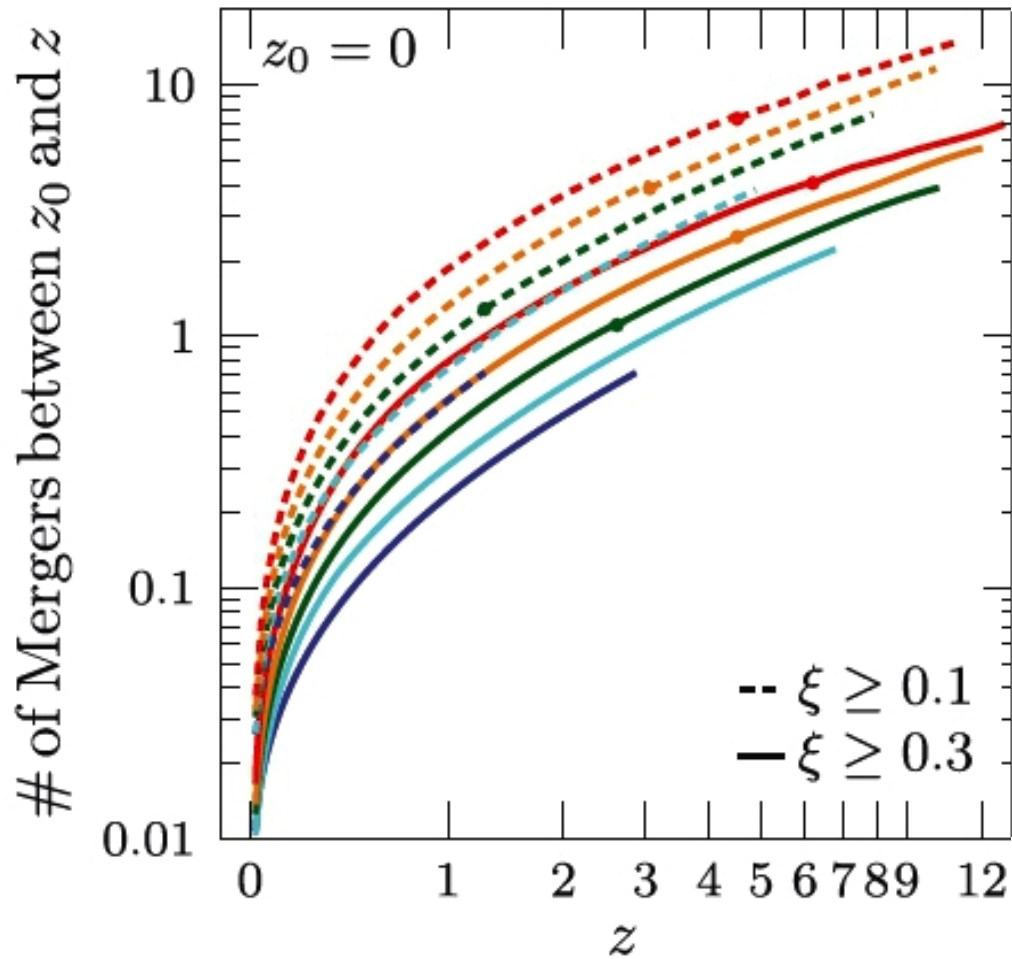# Mass and redshift dependence of the merging rate

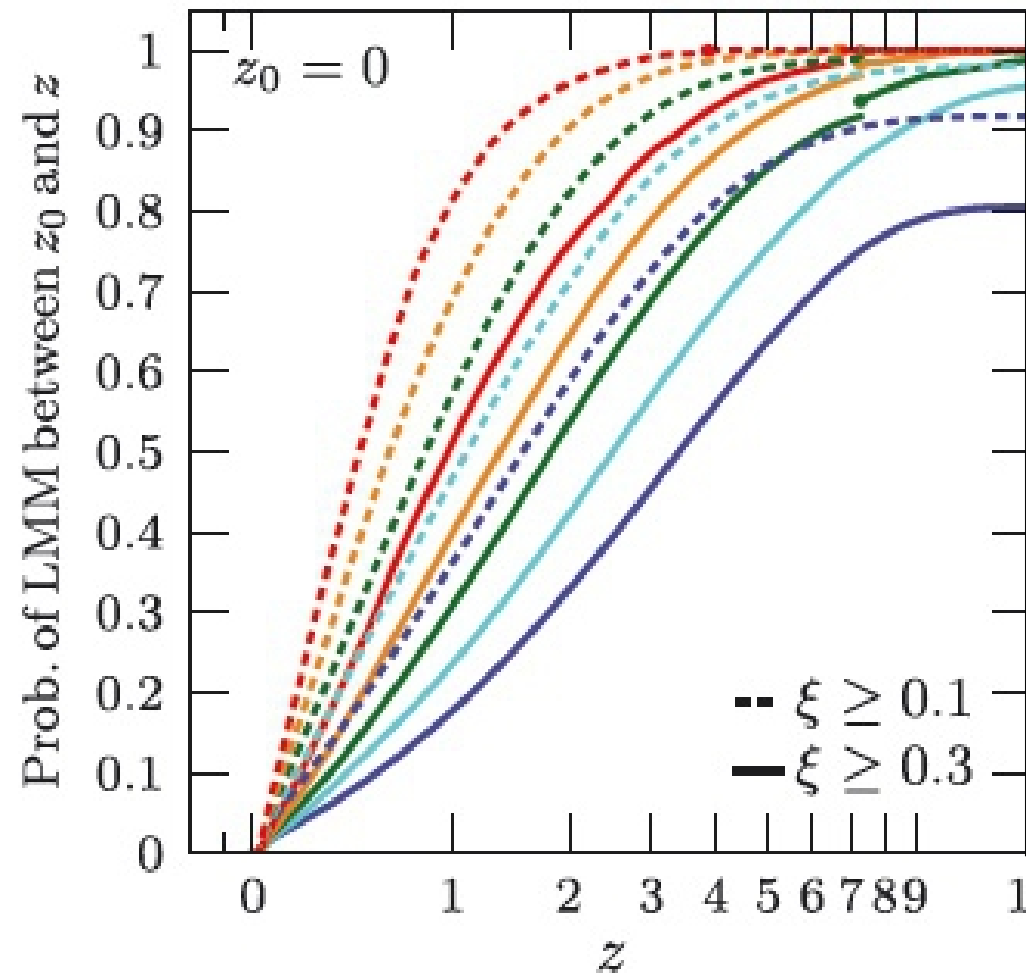# Mass growth of the largest progenitor as a function of z

$$\langle \dot{M} \rangle_{\mathrm{mean}} = 46.1\ \mathrm{M_\odot\ yr^{-1}} \left(\frac{M}{10^{12}\,\mathrm{M_\odot}} \right)^{1.1}$$

$$\times (1 + 1.11z)\sqrt{\Omega_{\mathrm{m}}(1+z)^3 + \Omega_\Lambda},$$
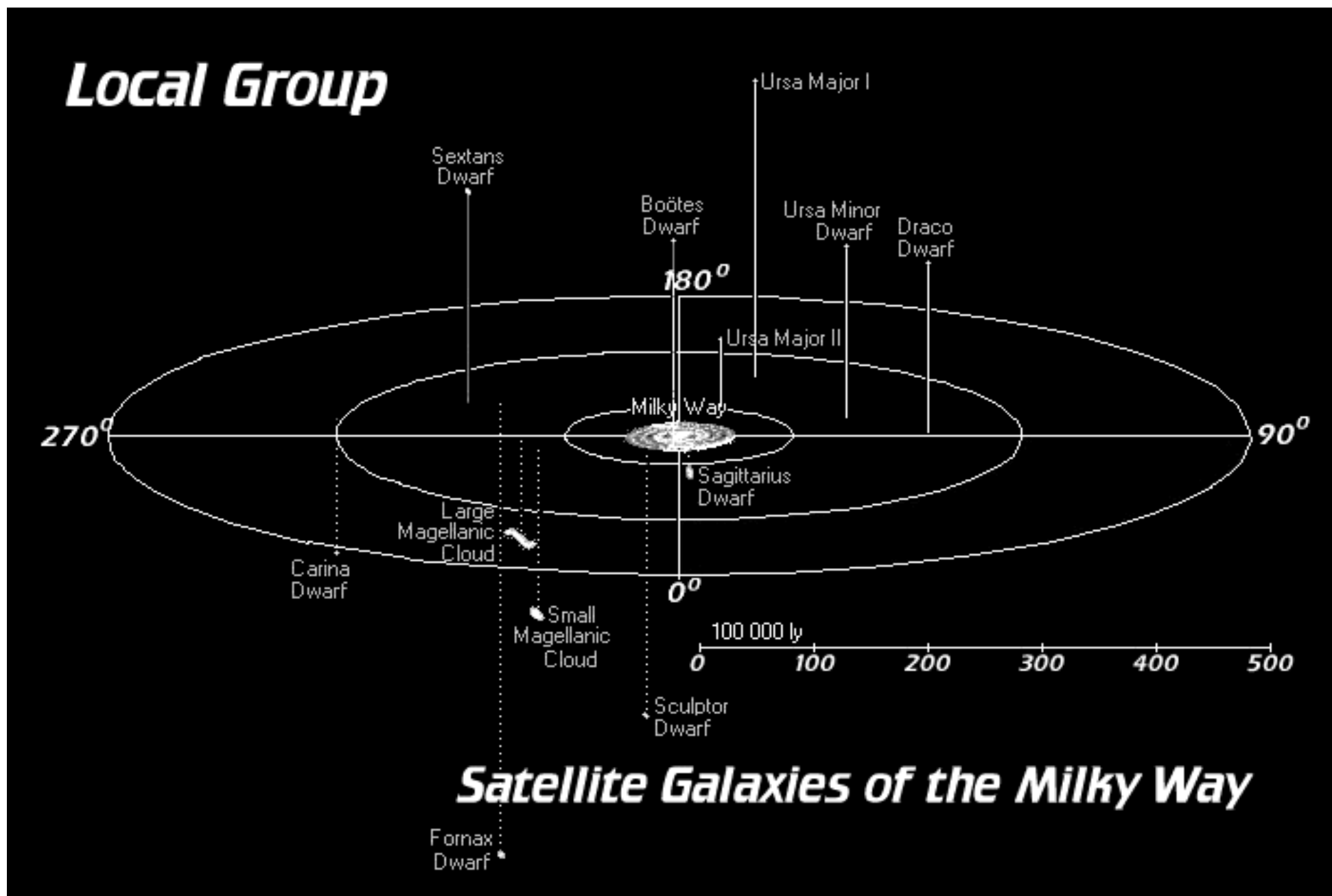
Cumulative number of mergers between redshift z and now

Probability of the last major merger having occurred between redshift z and now.

Massive halos are red, low mass halos are blue/purple.

The NFW profile can be turned into a velocity profile using
$V = (GM(r)/r^2)^{1/2}$

$$\left(\frac{V_c(r)}{V_{200}}\right)^2 = \frac{1}{x}\frac{\ln(1+cx) - (cx)/(1+cx)}{\ln(1+c) - c/(1+c)},$$

Where $x = r/r_{200}$ is the radius in units of the virial radius. Circular velocities rise near the center, reach a maximum (V_{max}) at $x_{max} \sim 2/c$, and decline near the virial radius. More centrally concentrated halos are characterized by higher values of V_{max}/V_{200}.
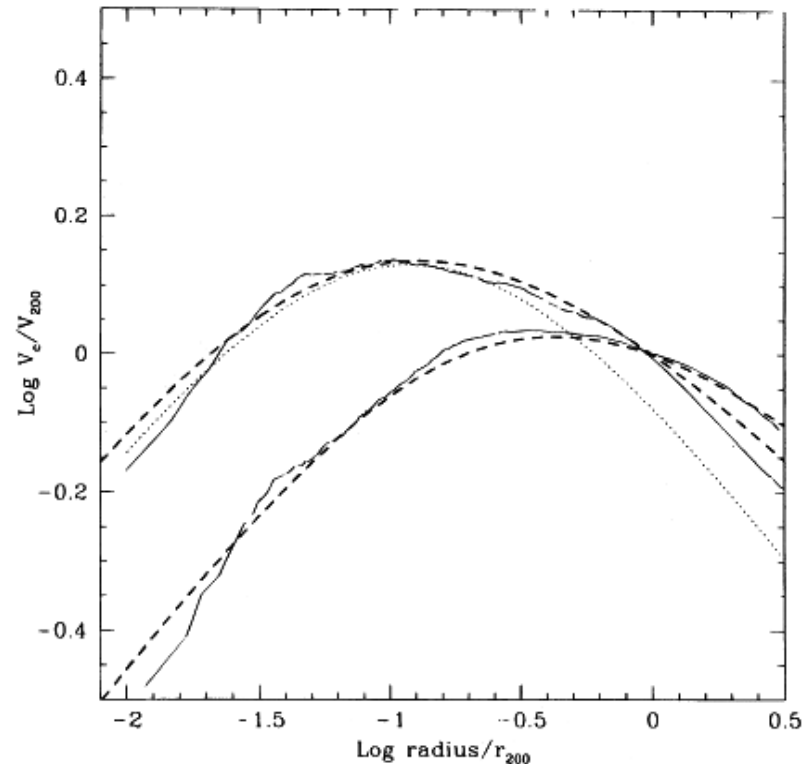
We use the Aquarius simulations to show that the most massive subhaloes in galaxy-mass dark matter (DM) haloes in Λ cold dark matter (ΛCDM) are grossly inconsistent with the dynamics of the brightest Milky Way dwarf spheroidal galaxies. While the best-fitting hosts of the dwarf spheroidals all have $12 \lesssim V_{max} \lesssim 25 \, km \, s^{-1}$, ΛCDM simulations predict at least 10 subhaloes with $V_{max} > 25 \, km \, s^{-1}$. These subhaloes are also among the most massive at earlier times,
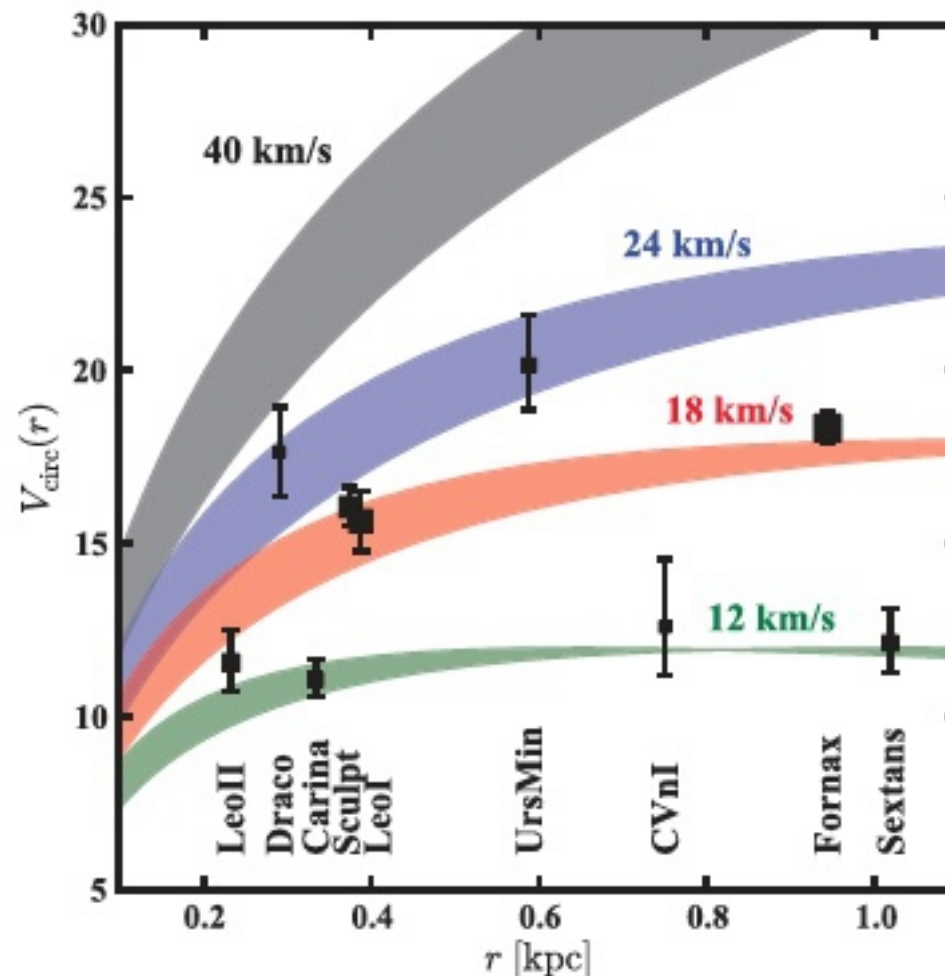
Same problem for M31
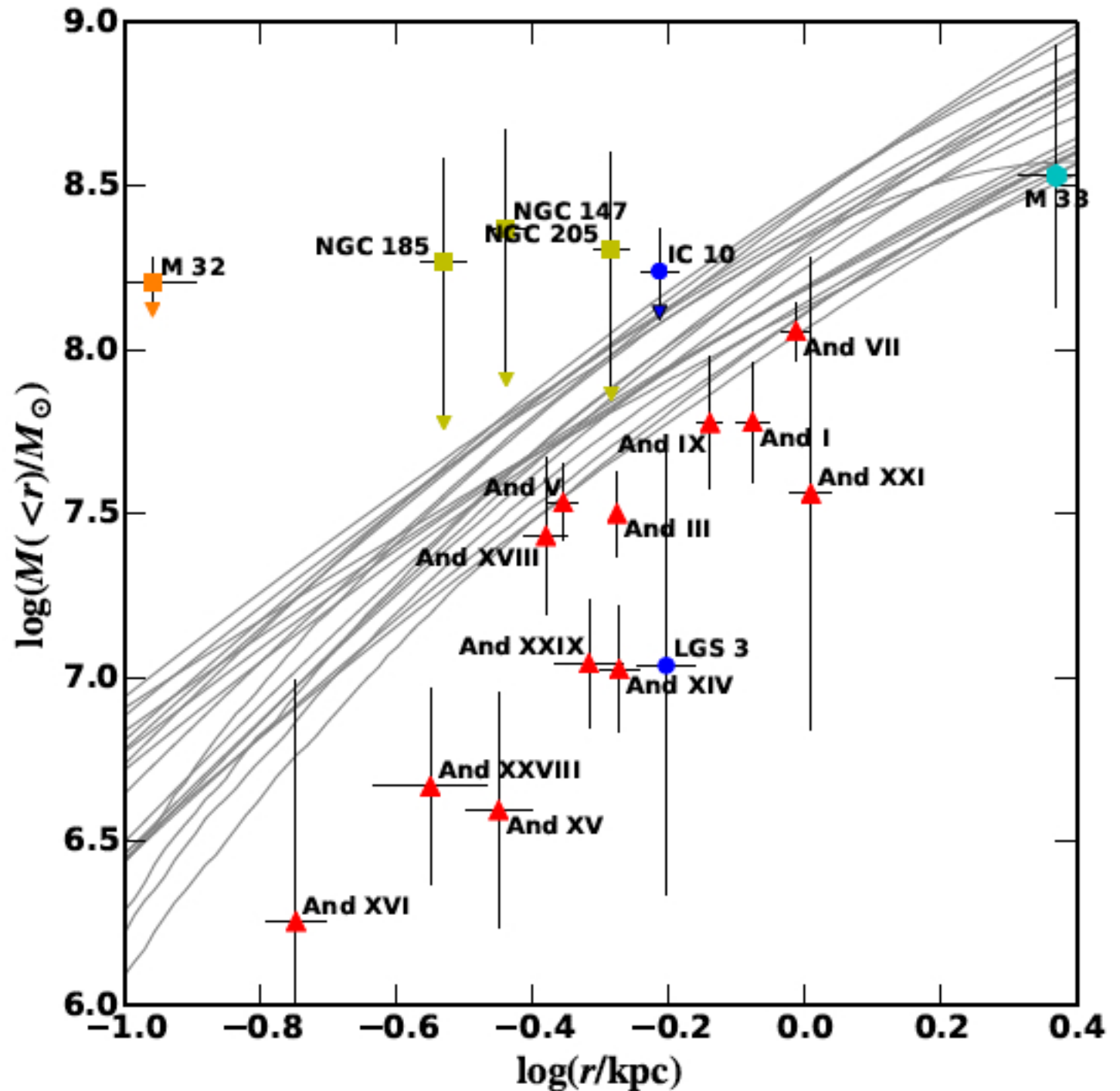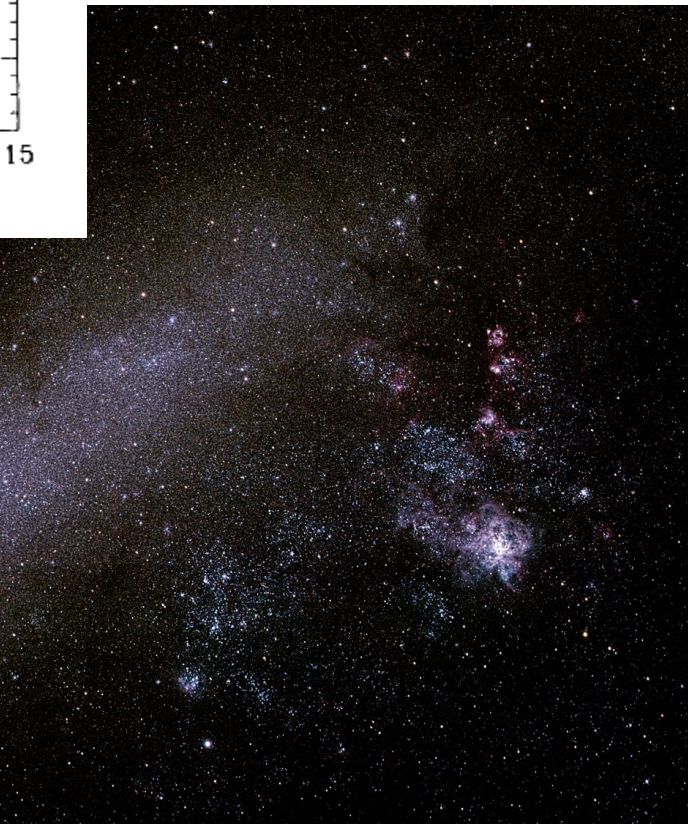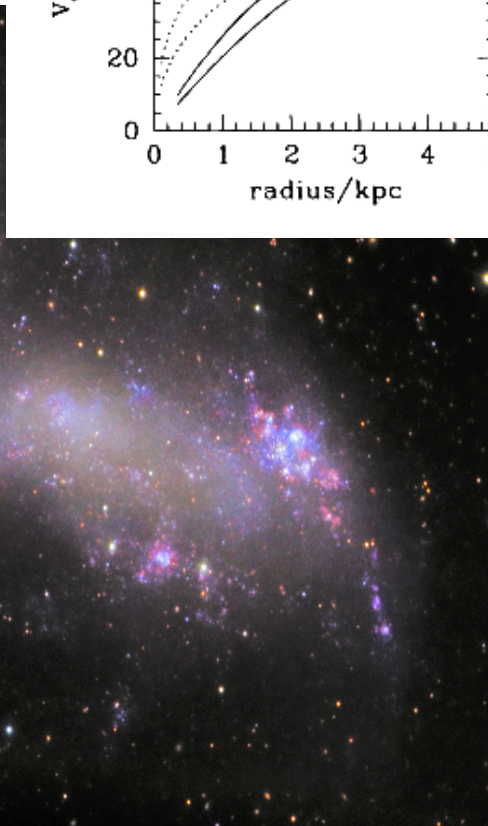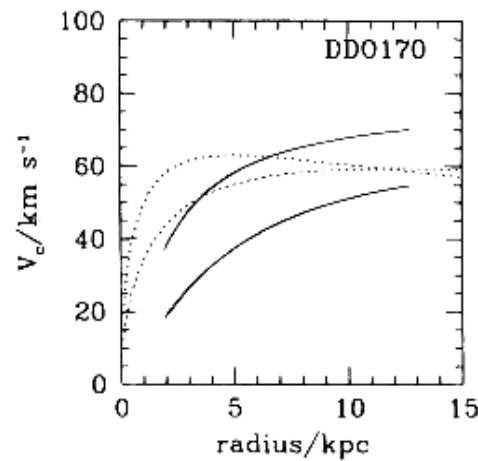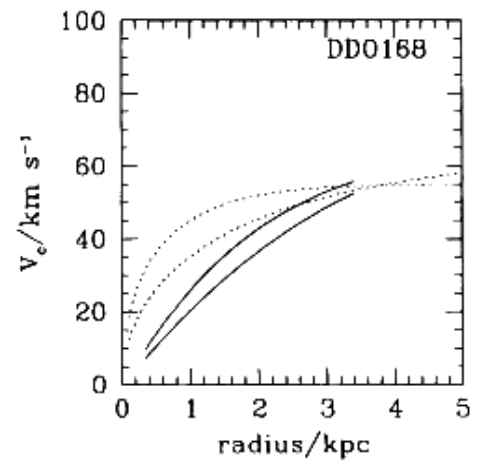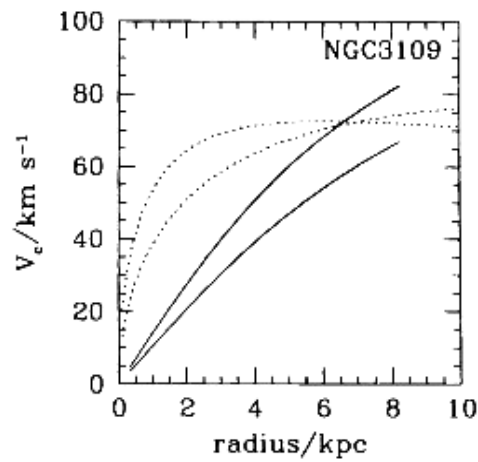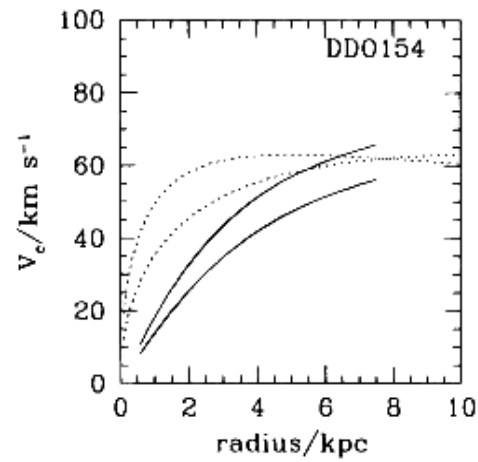
We conclude that, although the cores of dwarf galaxies pose a significant problem for CDM, the problem is not as bad as previously thought. Perturbations to the central regions of dwarf galaxy halos, resulting perhaps from the sudden loss of a large fraction of the baryonic material after a vigorous bout of star formation (Dekel & Silk 1986), can in principle reconcile the observations of dwarfs with the structure of CDM halos (Navarro, Eke, & Frenk 1995a).

But can this work in practice?